

ESTIMATES OF SOME THERMODYNAMIC  
PROPERTIES OF SALTS OF ALKALI  
METAL ANIONS AND A  $^{23}\text{Na}$  NMR  
STUDY OF EXCHANGE RATES  
IN METAL SOLUTIONS

Thesis for the Degree of M. S.  
MICHIGAN STATE UNIVERSITY  
CHARLES WESLEY ANDREWS  
1975

THESIS



ESTIMATES OF SOME THERMODYNAMIC PROPERTIES

OF SALTS OF ALKALI METAL ANIONS AND A

$^{23}\text{Na}$  NMR STUDY OF EXCHANGE RATES

IN METAL SOLUTIONS

By

Charles Wesley Andrews

ABSTRACT

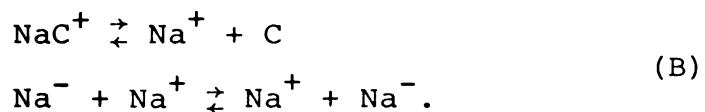
Extensive use was made of Born-Haber type calculations in order to estimate thermodynamic properties of the salts of the alkali metal anions. One cycle used to illustrate the ease with which  $\text{M}^-$  forms involved the formation of a hypothetical salt  $\text{M}^+\text{M}^-$  by the process  $2\text{M}_\text{s} \rightarrow \text{M}^+\text{M}^-$ . The most reasonable values for the enthalpy of formation indicate that since a crystalline salt which contains  $\text{Na}^-$  has been synthesized, such solid salts should be possible for all of the other alkali metals as well provided the cation can be suitably stabilized. A second cycle was employed in which the enthalpy change was estimated for the reaction  $2\text{M}_\text{s} + \text{C}_\text{s} \rightarrow \text{MC}^+\text{M}^-$ , in which C is a cryptand complexing agent. However, several terms in this cycle could be evaluated only by using additional energy cycles and questionable assumptions. This led to the use of a more reliable "difference calculation". The difference calculation invoked

a stability criterion in which the alkali anion salts ( $MC^+M^-$ ) were compared to a reference salt,  $NaC^+Na^-$ , which is known to be stable. In the reference salt, C represents 2,2,2 Cryptand ( $C_{222}$ ). The stability criterion is  $\Delta G_M^O - \Delta G_{Na}^O = \Delta H_M^O - \Delta H_{Na}^O - T (\Delta S_M^O - \Delta S_{Na}^O) \leq 0$  in which M and Na represent the salts  $MC^+M^-$  and  $NaC^+Na^-$ , respectively. Results of this difference calculation indicate that except for  $CsC_{222}^+Cs^-$  all the alkali metals should be able to form salts which contain anions of the alkali metals. The calculation in the case of the lithium salt involved 2,1,1 cryptand.

The NMR investigation utilized 18-crown-6 (18-C-6) to study the exchange of  $Na^-$  with  $NaC^+$  via NMR. Unlike metal solutions which contain  $NaC_{222}^+Na^-$  and are in the slow exchange limit between  $0^\circ$  and  $-40^\circ C$ , solutions which contain 18-C-6, Na, and methylamine are exchange-broadened and the  $NaC^+$  and  $Na^-$  peaks coalesce at  $-5^\circ C$ . The line shapes of the  $NaC^+$ ,  $Na^-$  spectra were fit with a generalized nonlinear least squares program to determine the exchange time  $\tau$ . The variation of  $\tau$  with temperature and the concentration of various species permits the exchange pathways to be examined. While the results are very preliminary at this stage, two mechanisms appear to be competing in the  $NaC^+$ ,  $Na^-$  exchange. They are



and



These mechanisms are qualitatively consistent with the fact that the exchange times and the apparent activation energies,  $E_a$ , are dependent upon the ratio  $[\text{Na}^-]/[\text{NaC}^+]$  as well as the presence of excess crown. The values for  $E_a$  range from  $18.2 \pm 0.3$  kcal mole<sup>-1</sup> for equimolar amounts of  $\text{Na}^-$  and  $\text{NaC}^+$  to  $25.2 \pm 1.2$  kcal mole<sup>-1</sup> when excess crown is present.

ESTIMATES OF SOME THERMODYNAMIC PROPERTIES  
OF SALTS OF ALKALI METAL ANIONS AND A  
 $^{23}\text{Na}$  NMR STUDY OF EXCHANGE RATES  
IN METAL SOLUTIONS

By

Charles Wesley Andrews

A THESIS

Submitted to  
Michigan State University  
in partial fulfillment of the requirement  
for the degree of  
MASTER OF SCIENCE  
Department of Chemistry  
1975

G 94406

To My Family  
For Their Prayers

## ACKNOWLEDGMENTS

The author wishes to express his appreciation to Professor James L. Dye for his guidance and encouragement as a teacher, a scientist, and a friend.

He would also like to thank Captain Steve Landers, USAF, and Joe Ceraso for their assistance with the NMR studies.

The author would also like to acknowledge Mike DaGue, Elizabeth Mei, Guan-Huei Ho, and Mike Yemen for their friendship and assistance.



## TABLE OF CONTENTS

Chapter	Page
LIST OF TABLES. . . . .	vi
LIST OF FIGURES . . . . .	viii
CHAPTER 1 - Historical. . . . .	1
The Nature of Alkali Metal Solutions. . . . .	2
The Alkali Anion . . . . .	3
The Role of Complexing Agents. . . . .	4
The Role of NMR Studies. . . . .	6
CHAPTER 2 - Experimental. . . . .	11
Instruments. . . . .	12
Data Analysis. . . . .	12
Chemical and Solvent Purification. . . . .	14
Sample Preparation . . . . .	15
Temperature Measurement. . . . .	15
CHAPTER 3 - Thermodynamic Considerations of Alkali Anion Formation . . . . .	18
Rationale. . . . .	19
A Hypothetical Salt. . . . .	19
Complete Born-Haber Cycle for $MC^+M^-$ Formation. . . . .	23
Enthalpy of Cryptand Sublimation . . . . .	26
Enthalpy of the Gas Phase Reaction . . . . .	27
Lattice Energy . . . . .	30
A Difference Calculation of the Born-Haber Cycle . . . . .	33

Chapter	Page
Discussion. . . . .	36
Possible Experimental Verification of the Thermodynamic Cycles . . . . .	40
CHAPTER 4 - NMR Exchange Studies of Alkali Metal Anion Solutions . . . . .	43
Rationale . . . . .	44
Three Site Exchange Processes . . . . .	47
Reduction of the Three-site Equa- tions to Two-site Equations . . . . .	50
Information From Non-Exchanging Systems . . . . .	54
18-C-6 Salt Exchange System . . . . .	56
Results of Na <sup>-</sup> , 18-C-6 Exchange Studies . . . . .	59
Uses of Other Complexing Agents . . . . .	63
Discussion of Results . . . . .	74
REFERENCES . . . . .	78

## LIST OF TABLES

Table		Page
1	Qualitative Trends in Metal Solution Equilibria . . . . .	7
2	Results for Hypothetical Salt Calculation. . . . .	24
3	Results of Energy Cycle Used to Determine the Enthalpy of the Gas Phase Reaction . . . . .	31
4	Results of Born-Haber Cycle Calcula- tion for $MC^+M^-$ Formation . . . . .	34
5	Results of the Difference Calcula- tion Using the Stability Criterion . . . . .	37
6	Possible Exchange Mechanisms and Expressions for $1/\tau_B'$ . . . . .	53
7	The Variation of the Linewidth and Chemical Shift of the Free and Com- plexed $^{23}\text{Na}$ Cation with Temperature. . . . .	55
8	The Variation of the Chemical Shifts, $\Delta$ , and the Transverse Relaxation Times, $T_2$ for 18-C-6, NaI Exchanging System. Concentrations of Complexed and Free Sodium Ions are Equal. . . . .	58
9	Composition of Samples Used for Line Shape Fitting . . . . .	60

Table	Page
10	The Temperature Dependence of the Exchange Time $\tau$ and $1/\tau_B$ for Sample 1 . . . . . 64
11	The Temperature Dependence of the Exchange Time $\tau$ and $1/\tau_B$ for Sample 2 . . . . . 65
12	The Temperature Dependence of the Exchange Time $\tau$ and $1/\tau_B$ for Sample 3 . . . . . 66
13	The Temperature Dependence of the Exchange Time $\tau$ and $1/\tau_B$ for Sample 4 . . . . . 67
14	The Temperature Dependence of the Exchange Time $\tau$ and $1/\tau_B$ for Sample 5 . . . . . 68
15	Apparent Activation Energy and $1/\tau_B$ (0°C) for Alkali Anion to Complexed Cation Exchanging Systems. . . . . 70
16	The Variation of the Linewidth and Chemical Shift With Temperature for Two Solutions Which Contain the 15-C-5 Complexing Agent and NaI. . . . . 71
17	The Variation of the Linewidth and Chemical Shift of $\text{NaC}^+$ and the Chemical Shift of $\text{Na}^-$ with Temperature for the 15-C-5 System in Methylamine . . . . . 73

## LIST OF FIGURES

Figure		Page
1	Examples of Two Classes of Complexing Agents . . . . .	5
2	Vessels for Sample Preparation A. For Air Sensitive Solutions B. Sealable NMR Tube for Salts . . . . .	16
3	Energy Cycle for a Hypothetical Solid Salt . . . . .	21
4	Born-Haber Cycle for $MC^+M^-$ Formation . . . . .	25
5	$^{23}\text{Na}$ NMR Spectra of $\text{Na}^+\text{C}_{222}$ and $\text{Na}^+$ (18-C-6), $\text{Na}^-$ in Methylamine . . . . .	45
6	$^{23}\text{Na}$ NMR Spectra of $\text{Na}^+$ (18-C-6), $\text{Na}^-$ in Methylamine at Various Temperatures . . . . .	46
7	Semilog Plot of Transverse Relaxation Times vs Reciprocal Temperature for Free NaI (○) and a 1:1 Complex of NaI and 18-C-6 (□). The log of the Viscosity of Methylamine is Plotted for Comparison (●) . . . . .	57
8	Line Printer Plot of Sample 1 at +5.7°C and -15.9°C. . . . .	61
9	Line Printer Plot of Sample 1 at -26.4°C and -32.9°C. . . . .	62

10	Arrhenius Plots of $1/\tau_B$ vs Reciprocal Temperature for Sample 1 ( $\bullet$ ), Sample 2 ( $\circ$ ), Sample 3 ( $\square$ ), Sample 4 ( $\star$ ), and Sample 5 ( $\times$ ) . . . . .	69
11	$^{23}\text{Na}$ NMR Spectra of: A. Equimolar NaI and 15-C-5 in Methylamine B. 15-C-5, Na in Methylamine . . . . .	72
12	Plot of $1/\tau_B$ at $0^\circ\text{C}$ vs (A) $\text{Na}^-$ Concentra- tion (B) Population of $\text{Na}^-$ Site/Population of $\text{NaC}^+$ Site ( $P_C/P_B$ ) for Various Samples . . .	76

CHAPTER 1  
HISTORICAL

## The Nature of Alkali Metal Solutions

The discovery by W. Weyl in 1863 of solutions of alkali metals in ammonia opened up a new field of challenging chemistry that has to this day remained, in part, a mystery. Metal ammonia solutions are characterized by high metal solubility (5M-6M), large molar extinction coefficients, rapid cation-electron exchange, phase separation at high concentrations and low temperatures (for Li, Na, K, and Rb) and thermodynamic instability. These characteristics, coupled with the lack of agreement among theoreticians about a suitable model, illustrate the complex nature of metal ammonia solutions.<sup>1</sup> For example, at the time of this writing a controversy persists about the nature of the intermediate concentration range in metal ammonia solutions. One school describes this concentration range as a solution composed of microscopically inhomogeneous regimes in which the concentration fluctuates locally about either of two well-defined concentration values. Opposing their view are those who believe the intermediate range to be a region of continuous concentration change.<sup>2</sup>

In general, metal ammonia solutions are described by models which place reducing species in potential wells formed by solvent molecules. The exact number, and nature of these species, and how and when the trap is formed is still a matter of debate.

Metal-amine and metal-ether solutions are very different from metal-ammonia solutions. The former are characterized



by low solubility, distinct optical bands, greater instability, and the presence of a number of distinct species.<sup>3</sup> These differences make the study of amine and ether solutions worthwhile. For example, the identification of a monomer, M, (sometimes described as an ion pair between the solvated electron and the cation) and the alkali anion  $M^-$ , were made possible because of the clear-cut esr spectra of M and the metal-dependent optical absorption bands for  $M^-$ . If these species are present in ammonia solutions they give spectral peaks which are buried under other bands or in some other way do not yield distinct spectra.

### The Alkali Anion

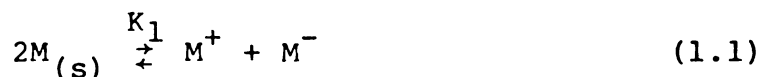
An interesting and controversial subject is the presence or absence of alkali anions in metal solutions. Although they were proposed a number of years ago for ammonia solutions there was no specific evidence for their existence and it was not until 1969 that Matalon, Golden, and Ottalenghi suggested that the metal-dependent visible bands observed in metal-amine solutions were due to  $Na^-$ ,  $K^-$ ,  $Rb^-$ , and  $Cs^-$  metal ions.<sup>4</sup> Much confusion about the metal-dependent bands existed prior to that time because of contamination by sodium from the Pyrex glass used to make up the solutions.<sup>5</sup> This contamination obscured the interpretation of the spectra for a long while.

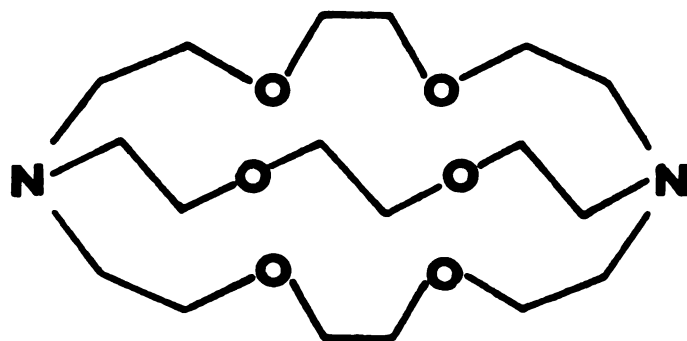
In addition to the evidence provided by the optical absorption band, there is now a host of other evidence which

verifies the existence of alkali anions. ESR measurements indicate the diamagnetic nature of this species and the conductance of  $M^-$  is very different from that of  $e^-_{\text{solv.}}$ . The Faraday effect, oscillator strength, and kinetics studies verify the stoichiometry of this species in amines and ethers.<sup>6</sup> The isolation and characterization of a crystalline salt of  $Na^-$  and the NMR spectrum of the  $M^-$  ion has caused the most excitement since these studies provided the most convincing argument for the existence of "genuine" alkali anions.<sup>7,8</sup>

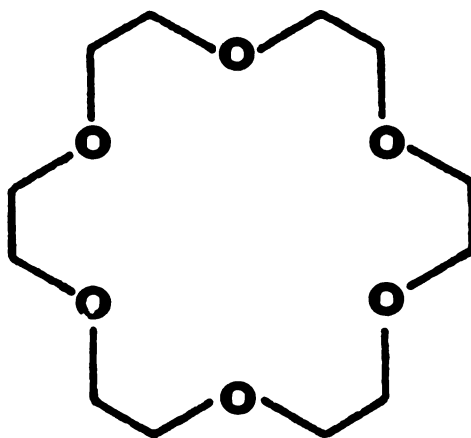
### The Role of Complexing Agents

When a complexing agent of the crown<sup>9</sup> or cryptand<sup>10</sup> class (see Figure 1) is added to a solution of an alkali metal in an amine or ether, the solubility of the metal is greatly increased. This increase in solubility is caused by the ability of the cyclic polyether to complex the alkali cation. This technique was suggested by V. A. Nicely<sup>11</sup> when he noted that many salts in the presence of a crown cyclic polyether dissolve in nonaqueous solvents in which they are normally insoluble. The effect of the crown and cryptand on the equilibrium among the various species present in the amines and ethers is clearly shown by the following set of equilibria:





1

**2,2,2 Cryptand****(C<sub>222</sub>)**

2

**18-Crown-6****(18-C-6)**

Figure 1. Examples of Two Classes of Complexing Agents.



In general the equilibrium constants are not known and are very difficult to obtain. However, certain trends as listed in Table 1 can be established on the basis of the solubility, optical spectra and esr spectra.

The proper choice of the type and concentration of the complexing agent in many cases permits one to tailor the nature of the solutions to meet his need. In general the cryptand gives a higher metal solubility than the corresponding crown compound. The symmetry of the complex also appears to be an important factor in both crystal growth and NMR spectroscopy. When crown complexes are formed, the interaction of the bound cation and the solvent is much greater than for cryptates. This can cause large solvent effects and lead to inclusion of solvent in many of the solid complexes. Similarly, the alkali metal NMR line is greatly broadened as a result of the asymmetric electric field gradient present in most crown complexes.

### The Role of NMR Studies

A major breakthrough came in 1974 when Dye and Ceraso reported the NMR spectrum of the sodium anion in tetrahydrofuran and in ethylamine.<sup>13</sup> Previously, only the paramagnetic

Table 1. Qualitative Trends in Metal Solution Equilibria

Reaction	Effect of Solvent <sup>a</sup> on Equilibrium Constant	Order of Decreasing Equilibrium Constant
(1) $M(s) \xrightleftharpoons{K_1} M^+ + e^-$	Decrease	Li, Cs, Rb, K, Na
(2) $M^+ + 2e^- \xrightleftharpoons{K_2} M^b$	Increase	Cs, Rb, K, Na, (Li) <sup>c</sup>
(3) $M^+ + 2e^- \xrightleftharpoons{K_3} M^-$	Increase	Na, K, Rb, Cs, (Li) <sup>d</sup>
(4) $M^+ + C \xrightleftharpoons{K_4} M^+C$	Unknown but expected to Increase	Depends upon nature of C

<sup>a</sup>Solvent Order:  $NH_3$ , HMPA, MA  $\sim$  EDA, EA, THF, DEE.

<sup>b</sup>M refers to the monomer species which gives hyperfine splitting in the ESR spectrum.

<sup>c</sup>No Li hyperfine splitting has been observed.

<sup>d</sup> $Li^-$  has not been observed.

shift (Knight shift) of the alkali cations could be studied due to solubility problems.<sup>14,15</sup> This recent study showed that the alkali metal anions in solution are indeed centrosymmetric species with two electrons in the outer s orbitals. This conclusion was based on two factors. First, the very small shift of the  $\text{Na}^-$  peak in solution from that of  $\text{Na}_{(\text{gas})}$  indicates that the p electrons are well shielded. Second, the narrow line width of  $\text{Na}^-$  indicates a spherical field gradient about the species.

One use of NMR techniques which is growing in importance is the determination of reaction rates. Lehn recognized the importance of proton NMR techniques for the study of cation exchange rates between the solvated and the cryptated states.<sup>16</sup> Shchori and co-workers extended this type of work further with a  $^{23}\text{Na}$  NMR kinetics study of sodium cation exchange in methanol, dimethoxyethane and N,N-dimethylformamide in the presence of dibenzo-18-crown-6.<sup>17,18</sup> More recent work by Dye and Ceraso, who first observed separate lines from sodium in two different environments, established the techniques which have been used in this laboratory<sup>19</sup> and provide the background for the NMR work in this thesis.

The basis for NMR rate studies is a set of phenomenological equations proposed by Bloch and modified by McConnell. The modified Bloch equations are:

$$\frac{dG_A}{dt} + \alpha_A B_A = -i\gamma H_1 M_{OA} + \tau_B^{-1} G_B - \tau_A^{-1} G_A \quad 1.5$$

$$\frac{dG_B}{dt} + \alpha_B G_B = -i\gamma H_1 M_{0A} + \tau_A^{-1} G_A - \tau_B^{-1} G_B \quad 1.6$$

in which  $G_A$  and  $G_B$  are the complex magnetizations caused by the nucleus in sites A and B, respectively. The definition of  $\alpha_A$  is  $\alpha_A = T_{2A}^{-1} - i(\omega_A - \omega)$  in which  $T_{2A}$  is the transverse relaxation time of nucleus A and  $\omega_A$  is the corresponding Larmor frequency;  $\alpha_B$  is similarly defined.  $H_1$  is the amplitude of the R.F. magnetic field and  $\gamma$  is the magnetogyric ratio of the nucleus being studied. Equations 5 and 6 are different from the original Bloch equations in that they allow for exchange. The  $\tau_A^{-1}$  term is the probability per unit time that a nucleus in position A will jump to position B. That is,  $\tau_A$  is the mean lifetime in position A.  $\tau_B$  has the same definition for position B. If needed, a third site can be added. This possibility will be discussed later.

The solution to equations 5 and 6 which is used in this work is as follows.

$$G = \left[ \frac{UT - SV}{S^2 + T^2} \right] \gamma H_1 M_0 - i\gamma H_1 M_0 \left[ \frac{SU + TV}{S^2 + T^2} \right] \quad 1.7$$

where

$$S = \frac{P_A}{T_{2A}} + \frac{P_B}{T_{2B}} + \frac{\tau}{T_{2A}T_{2B}} - \tau(\omega_A - \omega)(\omega_B - \omega) \quad 1.8$$

$$U = 1 + \tau \left( \frac{P_B}{T_{2A}} + \frac{P_A}{T_{2B}} \right) \quad 1.9$$

$$T = (P_A^{\omega_A} + P_B^{\omega_B - \omega}) + \tau \left( \frac{\omega_A - \omega}{T_{2B}} + \frac{\omega_B - \omega}{T_{2A}} \right) \quad 1.10$$

$$V = (P_B^{\omega_A} + P_A^{\omega_B - \omega}) \quad 1.11$$

and

$$\tau = \frac{\tau_A \tau_B}{\tau_A + \tau_B} \quad 1.12$$

This solution describes the line shape function in the general case, even when the transverse relaxation times in the two sites are different.

In the absence of exchange, the single complex moment is described by:

$$\frac{dG}{dt} + \left[ \frac{1}{T_2} - i(\omega_0 - \omega) \right] G = i\gamma H_1 M_0$$

The solution to this equation is:

$$G = \frac{KT_2^2(\omega_0 - \omega)}{1 + T_2^2(\omega_0 - \omega)^2} + i \left[ \frac{KT_2}{1 + T_2^2(\omega_0 - \omega)^2} \right]$$

These line-shape functions allow complete line-shape fitting to be done on the experimental data. Although there are examples of this method in the literature,<sup>22</sup> it has seldom been applied to such complex NMR data or as routinely as in this laboratory.



**CHAPTER 2**  
**EXPERIMENTAL**

## Instruments

The  $^{23}\text{Na}$  NMR spectra were obtained with an NMRS-MP-1000 spectrometer which uses a Varian DA-60 magnet, a lock system built in our lab, and a Nicolet 1083 computer system. The computer system allowed the use of pulsed fourier-transform techniques and permitted data to be punched directly onto paper tape for analysis with a CDC 6500 computer.\* The stability of the lock system (less than 2 Hz drift per hour) made it possible to take a reference spectrum only at the beginning and end of each series of temperature runs. The reference sample was measured at 25°C.

## Data Analysis

The Nicolet 1083 computer and an ASR-33 Teletype were used to punch the raw data onto paper tape as octal numbers. Computer cards were then punched from the octal tape and converted<sup>23</sup> to a second set of cards as decimal numbers with the proper format for the curve fitting program.

The NMR spectra line shapes were fit in most cases with five parameters using a generalized nonlinear least square program called "Kinfit".<sup>24</sup>

The form of the line shape function used to fit the two site exchange system follows.

---

\*For other details of the NMR system the reader is referred to the theses of David Wright and Joseph Ceraso, Michigan State University (1975).

$$G(\omega) = \frac{\gamma H_1 M_O}{S^2 + T^2} \{ (SU + TV) \cos(\theta_O + j \frac{\theta_1}{N}) - (UT - SV) \sin(\theta_O + j \frac{\theta_1}{N}) \} + C \quad 2.1$$

where

$$S = \frac{P_A}{T_{2A}} + \frac{P_B}{T_{2B}} + \frac{\tau}{T_{2A} T_{2B}} - \tau (\omega_A + \Delta - \omega) (\omega_B + \Delta - \omega) \quad 2.2$$

$$U = 1 + \tau \left( \frac{P_B}{T_{2A}} + \frac{P_A}{T_{2B}} \right) \quad 2.3$$

$$T = P_A (\omega_A + \Delta) + P_B (\omega_B + \Delta) - \omega + \tau \left( \frac{\omega_A + \Delta - \omega}{T_{2B}} + \frac{\omega_B + \Delta - \omega}{T_{2A}} \right) \quad 2.4$$

$$V = \tau [P_B (\omega_A + \Delta) + P_A (\omega_B + \Delta) - \omega] \quad 2.5$$

and

$$P_A = \frac{\tau_A}{\tau_A + \tau_B} \quad P_B = \frac{\tau_B}{\tau_A + \tau_B} \quad \tau = \frac{\tau_A \tau_B}{\tau_A + \tau_B} \quad 2.6$$

$T_{2A}$  and  $T_{2B}$  are natural relaxation times in absence of exchange.  $\omega_A$  and  $\omega_B$  are the Lamor frequencies in the absence of exchange. The five parameters which the computer adjusted were the amplitude ( $\gamma H M_O$ ), baseline (C), mean lifetime ( $\tau$ ) for exchange, the phase of the signal ( $\theta_O$ ) and the frequency shift ( $\Delta$ ) which adjusts  $\omega$  to compensate for frequency drift between sample and reference.  $T_{2A}$ ,  $\omega_A$ ,  $T_{2B}$  and  $\omega_B$  were measured in

separate experiments and entered as constants. The four other constants used in the line shape function were the second order phase correction ( $\theta_1$ ), number of points in digitalized spectra (N), and the population of the sites ( $P_A$  and  $P_B$ ). In several cases  $P_A$  was used as a sixth parameter when it could not be determined due to decomposition of the sample.

For the non-exchange systems in which  $\omega_A$ ,  $T_{2A}$ ,  $\omega_B$  and  $T_{2B}$  were determined the complete shape function is

$$G = \frac{KT_2}{1+T_2^2(\omega_0-\omega)^2} [\cos(\theta_0+\theta_1) - T_2(\omega_0-\omega)\sin(\theta_0+\theta_1)] \quad 2.7$$

The five parameters are the amplitude (K), C,  $T_2$ ,  $\omega_0$  and  $\theta_0$ . The two constants used are  $\theta_1$  and N.

### Chemical and Solvent Purification

Methylamine,  $\text{MeNH}_2$ , the solvent used, was purified by distilling it onto BaO where it was allowed to stand for several weeks with occasional freeze-pumping cycles.\* The  $\text{MeNH}_2$  was then distilled from BaO onto a fresh film of Na-K alloy where it was allowed to stand at room temperature with occasional freeze-pumping. The amount of decomposition at this stage was small as indicated by the amount of hydrogen formed. The  $\text{MeNH}_2$  was then distilled into a thick-walled

---

\* Methylamine was purchased from J. T. Baker Co.

storage vessel. All distillations were done after evacuation to a pressure of less than  $10^{-5}$  torr. Ethylamine was similarly purified.

18-crown-6 was recrystallized twice from acetonitrile and vacuum-dried.\* Its melting point was in the range of 38 - 40 degrees centigrade. The 2,2,2 cryptand was synthesized by a modification of Lehn's procedure.<sup>25</sup>

### Sample Preparation

All reactive metal solutions for the NMR experiments were prepared in specially cleaned<sup>25</sup> glass vessels of the design shown in Figure 2A. The metal solutions were saturated at 0°C for one half hour by allowing the solution to stand over a metal mirror and shaking the solution. The metal was purified by no fewer than three vacuum distillations. Less reactive salt solutions were prepared by quickly loading the dried, weighed sample into a sealable NMR tube (Figure 2B). The sealable tube was pumped to  $10^{-5}$  torr, the solvent distilled in, and then sealed off in the normal fashion.

### Temperature Measurement

The temperature was controlled with a Varian NMR temperature controller model number V-4540. The temperature was measured with a calibrated Doric digital readout thermocouple.

---

\* 18-crown-6 was purchased from PCR Incorporated.

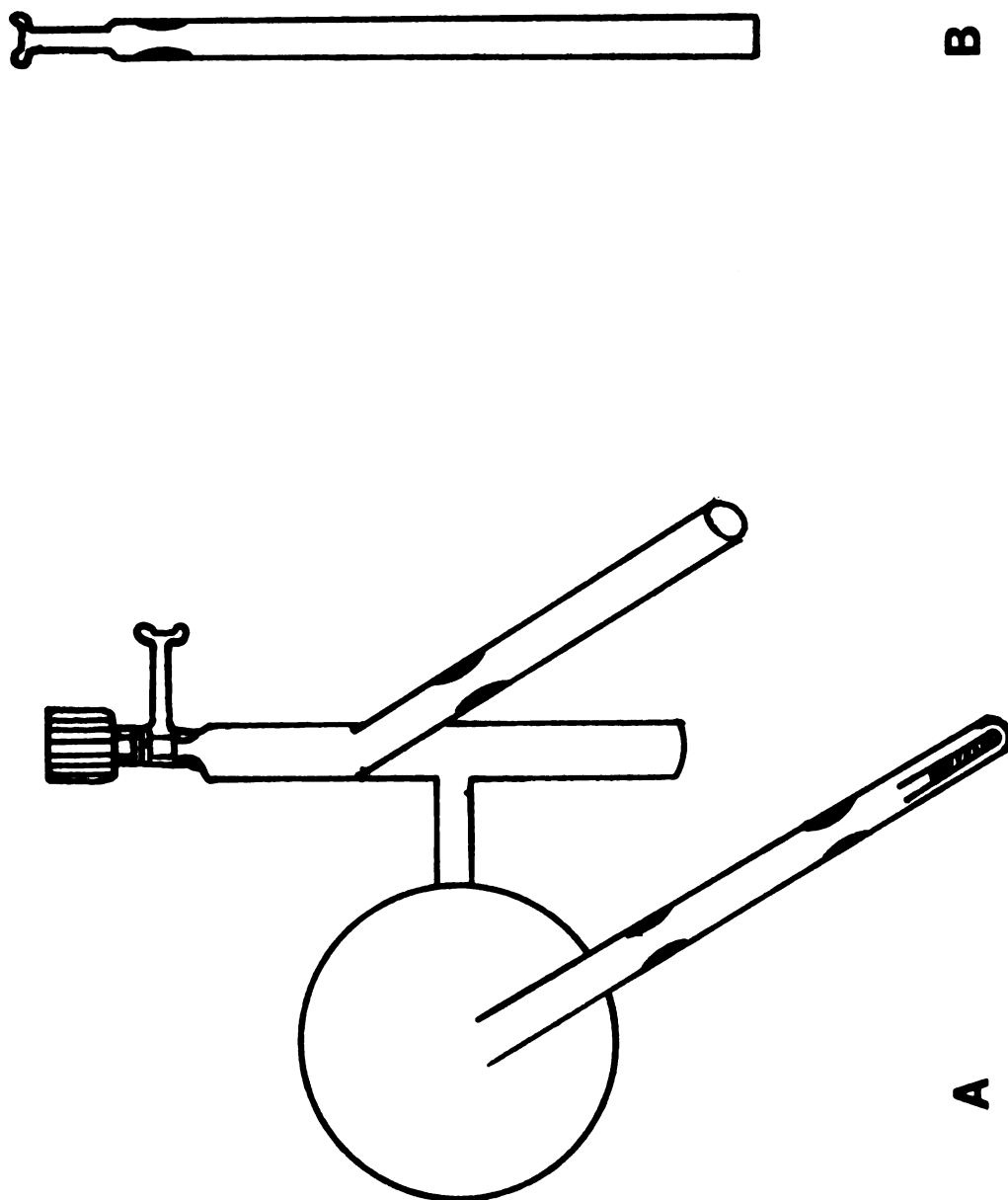


Figure 2. Vessels For Sample Preparation A. For Air Sensitive Solutions B.  
Sealable NMR Tube for Salts.

One thermocouple wire was placed approximately 1 cm below the 10 mm NMR tube in the probe. A second thermocouple wire was placed in the 10 mm tube containing 1 ml of isopropyl alcohol. A calibration plot of the temperature in the tube vs. the temperature below the tube was made. The plot was linear and reproducible to  $\pm 1^{\circ}\text{C}$ .

CHAPTER 3  
THERMODYNAMIC CONSIDERATIONS OF  
ALKALI ANION FORMATION



## Rationale

The evidence for alkali anions is very convincing; however, certain puzzling facts remain. One of the most intriguing is the absence of a lithium anion in any lithium solutions. Is this absence due to some anomalous thermodynamic behavior or simply that the right conditions have not been met? The second puzzling phenomenon is the fact that to date only one salt (of the sodium anion) has been produced by crystallization even though solutions which contain  $K^-$ ,  $Rb^-$ , and  $Cs^-$  can be readily prepared.

With these questions in mind, the thermodynamics of formation of the solid anion salts has been investigated. This information may then be used to predict the feasibility of compound formation and thermodynamic stability of salts of the alkali anions.

## A Hypothetical Salt

The alkali metals have certain properties which, taken together, make them unique among the elements. They have a low first ionization potential, positive electron affinity, and small heat of vaporization. All of these properties work together to make it relatively easy to form a salt which contains both cations and anions rather than neutral atoms. This is clearly illustrated by an energy cycle in which the alkali metal forms a hypothetical solid salt (H.S.) as shown

in Figure 3. Other than  $\Delta H_F$  the only term which is not known is the lattice energy. Several methods are available to calculate this term. However, most require a knowledge of the structure and other parameters of the salt. From the Born-Lande equation

$$U = \frac{NMZ_+Z_-e^2}{r} \left(1 - \frac{1}{n}\right) \quad 3.1^*$$

We know that the lattice energy varies as  $\frac{1}{r}$  from one salt to another. Therefore, the lattice energy of the hypothetical salt may be obtained from that of a reference salt of similar structure by the use of the multiplicative scaling factor  $r_{R.S.}/r_{H.S.}$ .

$$U_{H.S.} = U_{\text{Ref. salt}} \times \frac{r_{R.S.}}{r_{H.S.}} \quad 3.2$$

The difficulty is to choose the proper structure for the hypothetical salt so that an appropriate reference salt can be chosen, and to predict the radius of the hypothetical salt. Three methods have been used for comparison.

The first method assumes the interatomic distance in the H.S. is the same as the interatomic distance in the metal except that structure of the H.S. is similar to the structure of sodium iodide. This is reasonable in view of X-ray

---

\* U is the lattice energy, N is Avogadro's number, M is the Madelung constant,  $Z_+$  and  $Z_-$  are the valences of the ions, e is the charge on the electron, r is the interatomic distance, and n is the electronic shell's repulsion exponent.

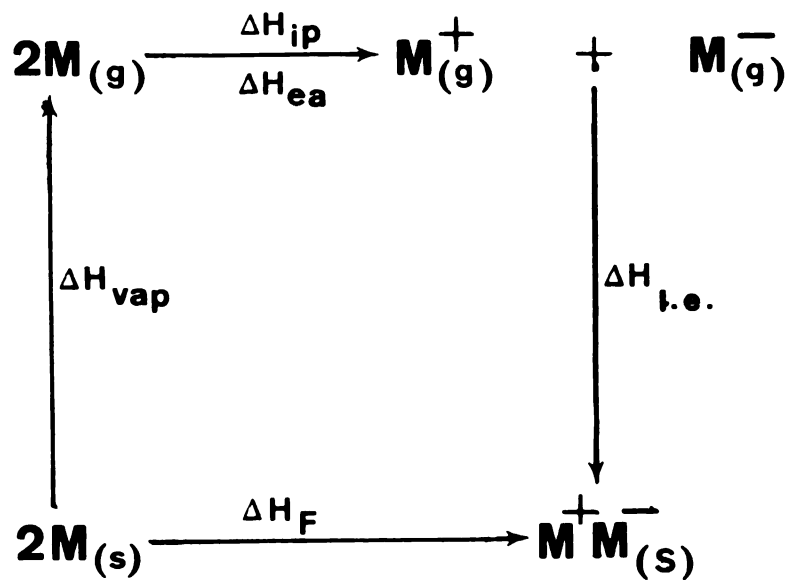


Figure 3. Energy Cycle for a Hypothetical Solid Salt.

measurements of the  $\text{NaC}^+\text{Na}^-$  solid which show that the radius of  $\text{Na}^-$  is approximately equal to the radius of  $\text{I}^-$ . This causes the radius ratio, an important factor in determining crystal packing, to be about the same for  $\text{Na}^+/\text{I}^-$  and  $\text{Na}^+/\text{Na}^-$ . Hence, the lattice energy of sodium iodide is scaled by a factor of  $r_{\text{M}^+\text{M}^-}/r_{\text{Na}^+\text{I}^-}$  where  $r_{\text{M}^+\text{M}^-}$  and  $r_{\text{Na}^+\text{I}^-}$  are the interatomic distances in the metal and salt respectively.

The second model used to calculate the lattice energy of the H.S. is to keep the density of the H.S. the same as the density of the metal but change the crystal structure from a body-centered cubic (metal) to a face-centered cubic (salt). This then has the effect of changing the interatomic distance to maintain the same density in the transition from metal to H.S. salt. The NaI lattice energy is still used. This is illustrated when we recall that the alkali metals form a B.C.C. lattice with two atoms per unit cell.

$$\text{Volume per atom} = \frac{1}{2} a^3 = \frac{4}{\sqrt{27}} r_{\text{B.C.C.}}^3 = V_{\text{M}^+\text{M}^-} \quad 3.3$$

where  $a$  is the length of the unit cell and  $r$  is the interatomic distance. If this structure is changed to a F.C.C. with the same density, we then have

$$V_{\text{M}^+\text{M}^-} = \frac{1}{8} a_{\text{F.C.C.}}^3 = r_{\text{F.C.C.}}^3 \quad 3.4$$

or

$$r_{\text{F.C.C.}} = r_{\text{B.C.C.}} \left( \frac{4}{\sqrt{27}} \right)^{1/3} \quad 3.5$$

The scale factor then becomes

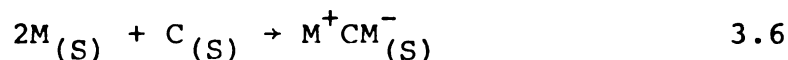
$$r_{\text{Na}^+\text{I}^-}/r_{\text{B.C.C.}} \left(\frac{4}{\sqrt{27}}\right)^{1/3}$$

The third model used to calculate the lattice energy of the H.S. assumes that both the interatomic distance and the lattice structures of the H.S. stay the same as that of the metal. This structure was then scaled using a CsCl lattice energy. CsCl of course has a B.C.C. lattice. This model is not as reasonable as the first two but it serves a purpose in that it allows comparison with the first two models.

The results of these calculations are shown in Table 2 for all the alkali metals along with some of the data used in the calculations.

#### Complete Born-Haber Cycle for $\text{MC}^+\text{M}^-$ Formation

A more complete understanding of the thermodynamics can be achieved by using an energy cycle which considers a complexing agent such as a cryptand. One such cycle is shown in Figure 4 which represents the process



The terms in Figure 4 have the following meanings.  $\Delta H_{\text{vap}}$  is the heat of sublimation of the alkali metal,  $\Delta H_{\text{ip}}$  and  $\Delta H_{\text{ea}}$  are the enthalpy due to the ionization potential and the

Table 2. Results for Hypothetical Salt Calculation.

Enthalpy Change (kcal mole <sup>-1</sup> ) (See Figure 3)							
Metal	M-M distance <sup>1</sup> in Metal (Å)	$\Delta H_{\text{vap}}$ <sup>2</sup>	$\Delta H_{\text{ip}}$ <sup>2</sup>	$\Delta H_{\text{ea}}$ <sup>3</sup>	$\Delta H_{\text{f}}$ Model #1	$\Delta H_{\text{f}}$ Model #2	$\Delta H_{\text{f}}$ Model #3
Li	3.03	33.17	124.3	-17.8	0.4	-14.9	-21.8
Na	3.72	24.03	118.5	-12.5	10.2	-1.9	-7.7
K	4.5	19.35	100.1	-11.8	7.9	-1.7	-6.6
Rb	4.87	18.64	96.3	-11.1	11.9	3.6	-.9
Cs	5.42	16.82	89.7	-9.0	13.5	5.8	1.6

<sup>1</sup>C. S. Barrett, Structure Reports, 20 (1956).<sup>2</sup>Handbook of Chemistry and Physics, 50th Ed., Chemical Rubber Co., 1970.<sup>3</sup>E. M. Chen, W. E. Wentworth, J. Chem. Ed., 52, 486 (1975).

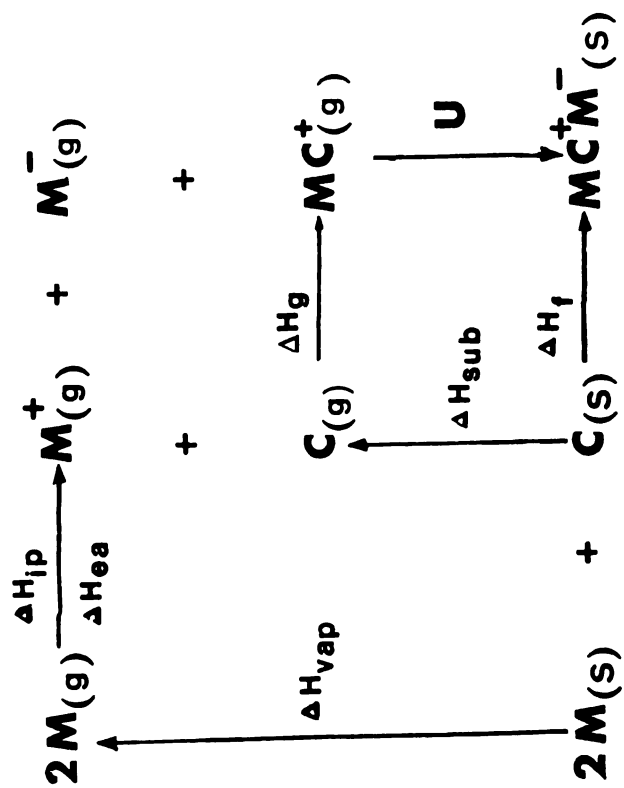


**Figure 4. Born-Haber Cycle for  $\text{MC}^+\text{M}^-$  Formation.**

electron affinity respectively,  $\Delta H_{\text{sub}}$  is the enthalpy of sublimation of the cryptand,  $\Delta H_g$  is the heat of formation of the gaseous complex between the cation and the cryptand, and lastly,  $U$  is the lattice energy of the solid compound. The terms which are not available from the literature are  $\Delta H_{\text{sub}}$ ,  $\Delta H_g$ , and  $U$ . Fortunately, some data are available which allow estimates to be made, but the reliability of these estimates is questionable. An attempt is made to evaluate these terms, point out possible errors, and finally to use these estimates to draw conclusions about the  $\text{MC}^+\text{M}^-$  salt.

### Enthalpy of Cryptand Sublimation

The enthalpy of sublimation of the cryptand was determined by neglecting the enthalpy of fusion and using Trouton's rule.

$$\overline{\Delta S}_{\text{vap}} = \frac{\Delta \overline{H}_{\text{vap}}}{T_b} \approx 21 \text{ cal/deg mol} \quad 3.7$$

where  $T_b$  is the boiling point of the compound.  $T_b$  was calculated by use of the Clausius-Claperyron equation

$$\log\left(\frac{p_2}{p_1}\right) = \frac{H_{\text{vap}}(T_2 - T_1)}{2.303R(T_2 T_1)} \quad 3.8$$

which relates the vapor pressure  $p$  to the absolute temperature  $T$  by means of the enthalpy of vaporization. The values of  $p_2$  and  $T_2$  are one atmosphere and the boiling temperature



respectively.  $p_1$  and  $T_1$  were calculated by using the Langmuir free-evaporation method<sup>26</sup> with sublimation data. In the Langmuir free-evaporation method, the rate of loss of mass ( $d\omega/dt$ ) by vaporization from a sample of area  $a$  in a vacuum is related to the equilibrium vapor pressure by the equation

$$p = \frac{(-d\omega/dt) (2\pi RT/M)^{1/2}}{a\alpha} \quad 3.9$$

The factor  $\alpha$  is the coefficient of evaporation and is often assumed to be unity.  $M$  is the molecular weight. One difficulty with this method is that the area ( $a$ ) is not easy to evaluate. The data used were as follows.

Weight of  $C_{222}$  evaporated = 0.7 g.

Temperature of vaporization =  $110^\circ\text{C}^*$

Duration of vaporization =  $2\frac{1}{2}$  hours

Surface area of material =  $3.14 \text{ cm}^2$

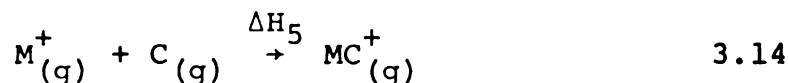
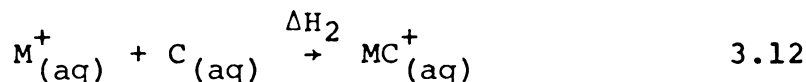
A value of  $22.1 \text{ kcal/mol}$  was obtained for  $\Delta H_{\text{sub}}$  by using this method.

### Enthalpy of the Gas Phase Reaction

The enthalpy of the gas phase reaction of metal and cryp-tand may be estimated by the following set of reactions.

---

\*This is above the melting point of  $C_{222}$ .



From these reactions it is clear that

$$\Delta H_5 = \Delta H_1 + \Delta H_2 + \Delta H_3 - \Delta H_4 \quad 3.15$$

Everything on the right hand side of this equation is known or can be calculated. For instance, the heat of hydration of the alkali metals is fairly well known<sup>27</sup> from both experimental work and theory. The heats of aqueous cryptation are small and are also known for most of the compounds used here.  $\Delta H_4$  was calculated by using a modification of the Born equation<sup>28</sup>

$$\Delta H_{\text{solv.}} = \frac{-Z^2 e^2 N_o}{8\pi \epsilon_o r_o} \left(1 - \frac{1}{D}\right) + T \frac{Z^2 e^2 N_o}{8\pi \epsilon_o r_o D^2} \left(\frac{\partial D}{\partial T}\right) \quad 3.16$$

in which  $Z$  is the valence of the ion,  $e$  the charge on the electron,  $N_o$  is Avogadro's number,  $\epsilon_o$  the permittivity of free space,  $r_o$  the radius of the ion and  $D$  the dielectric constant.

By using the values of these quantities with water as a solvent we have:

$$\Delta H = \frac{-166Z^2}{r_o} + T(.0094)\frac{Z^2}{r_o}\left(\frac{\text{kcal}}{\text{mole}}\right) \quad 3.17$$

Lehn introduced a technique for the evaluation of the radius of the complexed cation by adding the ligand thickness to the radius of the free ion.<sup>29</sup> The procedure used to determine the ligand thickness (s) consists of spreading the volume of the ligand around the cation and calculating the thickness of the layer. The value of the ligand thickness is given by:

$$s = \left(r_i^3 + \frac{3V_L}{4}\right)^{1/3} - r_i \quad 3.18$$

where  $r_i$  is the radius of the cation and  $V_L$  is the volume of the ligand.  $V_L$  is the sum of the Van der Waals volume of the atoms and groups forming the ligand.

One of the major problems with the Born equation is that the dielectric constant is not a constant as the Born equation assumes. It is a function of the field strength about the ion. However, two factors increase the validity of the Born equation in this case. First is that in a high dielectric constant medium where  $\epsilon/\epsilon_0 \gg 1$ , the errors will not be too serious and secondly, the radius of the cryptated cation is greater than 5.0 Å so that the electric field gradient is not

as high as for most bare ions.

In order to proceed with this calculation, a critical assumption had to be made about the enthalpy of transfer of cryptand from the gas phase to water ( $\Delta H_2$ ). The Born equation calculates only the free energy of solvation which is due to the electrostatic interaction of the ion. It neglects all the non-electrostatic terms. The assumption is made that the non-electrostatic term in  $\Delta H_4$  cancels the enthalpy of transfer for the cryptand ( $\Delta H_2$ ). There are problems with this assumption; the biggest is the fact that there are probably large conformational changes between the cryptand and the cryptate which will have a pronounced effect on the enthalpy of transfer. However, the magnitude of these effects is unknown and very hard to measure. If we assume that the error from one alkali cryptate to another is approximately the same, we can still use this result for our purposes. The results of this calculation are shown in Table 3. The difference calculation described later in this chapter will prove to be more reliable for doing this.

### Lattice Energy

The determination of the lattice energy of the cryptated anion salt poses another interesting problem. The classic method used to calculate the lattice energy of a salt is the Born-Landé equation which has already been mentioned. The problems with this equation, although it gives good results,

Table 3. Results of Energy Cycle Used to Determine the Enthalpy of the Gas Phase Reaction.

Metal Ion	Radius of Cryptated Cation (Å)	$\Delta H_1$ kcal mole <sup>-1</sup>	$\Delta H_3$ kcal mole <sup>-1</sup>	$\Delta H_4$ kcal mole <sup>-1</sup>	$\Delta H_5$ kcal mole <sup>-1</sup>
Li <sup>+</sup>	5.06*	-132.1	-4.6	-32.4	104.3
Na <sup>+</sup>	5.50	-106.0	-5.8	-29.8	-82.0
K <sup>+</sup>	5.52	-85.8	-11.1	-29.7	-67.2
Rb <sup>+</sup>	5.53	-79.8	-10.5	-29.6	-60.7
Cs <sup>+</sup>	5.56	-72.0	-2.0	-29.5	-44.5

\* Values for C<sub>2,1,1</sub> were used.

are two-fold. First, a certain crystal structure must be assumed before this equation can be used. Second, the calculation of the Madelung constant is a formidable task requiring much mathematical manipulation for complex structure types. A reasonable alternative to the Born-Lande equation is the Kapustinskii<sup>30</sup> equation

$$U = \frac{287.2v Z_+Z_-}{r_+ + r_-} = \left[ 1 - \frac{0.345}{r_+ + r_-} \right] \quad 3.19$$

where  $v$  is the number of ions in the chemical molecule,  $(r_+ + r_-)$  is used for  $r_0$  the interionic distance, and  $Z_+$  and  $Z_-$  are the valences of the ions.

Kapustinskii found that the Madelung constant, the internuclear distance, and the empirical formula of an ionic compound are all interrelated. This is not surprising when one considers that, given a certain number of ions of a certain size, the number of ways of packing them efficiently is limited. Calculation of rock salt type lattice energies by both the Kapustinskii and the Born-Lande equation gives results that are within a small percentage difference of one another in most cases.<sup>30,31</sup>

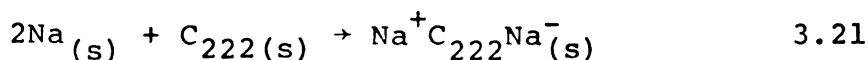
In calculating the values of the lattice energy for the alkali anion salts, the same value of the cation radius was used as in the previous calculation of  $\Delta H_4$ . The value of the radius of the anion was estimated by using the suggestion of Matelon, et al. in which

$$r_{M^-} = r_{M-M} - r_{M^+} \quad 3.20$$

In this equation  $r_{M^-}$  is the radius of the anion,  $r_{M-M}$  is the interatomic distance in the metal, and  $r_{M^+}$  is the ionic radius of the cation. Justification for the use of this anion radius is presented in the discussion of these results. The results of the complete Born-Haber cycle are shown in Table 4.

#### A Difference Calculation of the Born-Haber Cycle

Many of the problems of the previous thermodynamic cycles can be overcome by computing only energy differences in the cycles of the alkali cryptates and by using sodium cryptate as a reference. The sodium case is used because it is known that the sodium cryptate solid is a stable compound. We know that Equation 21



describes the formation of a stable gold-colored solid.

Therefore

$$\Delta G_{Na}^O = \Delta H_{Na}^O - T\Delta S_{Na}^O \leq 0 \quad 3.22$$

For other alkali cryptate salts of this type, the following could also be written.

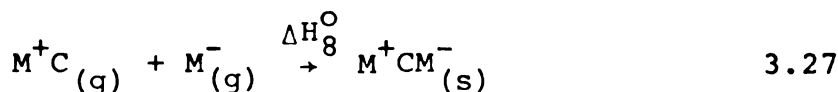
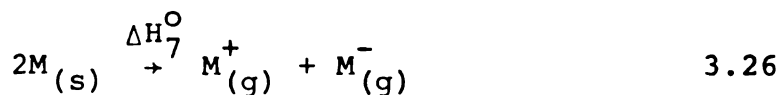
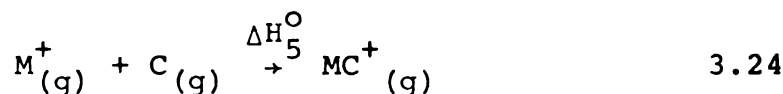
Table 4. Results of Born-Haber Cycle Calculation for  $MC^+M^-$  Formation.

Compound	Radius of Anion ( $\text{\AA}$ ) ( $2r_m - r_{m+}$ )	$U_{MC^+M^-}$ kcal mole $^{-1}$	$\Delta H_f$ kcal mole $^{-1}$
$LiC^+Li^-$	2.4	-73.	24.
$NaC^+Na^-$	2.8	-72.	35.
$KC^+K^-$	3.2	-64.	19.
$RbC^+Rb^-$	3.4	-63.	22.
$CsC^+Cs^-$	3.6	-60.	38.



$$\Delta G_M^O - \Delta G_{Na}^O = (\Delta H_M^O - \Delta H_{Na}^O) - T(\Delta S_M^O - \Delta S_{Na}^O) \leq 0 \quad 3.23$$

where M refers to a salt of  $MC^+M^-$  type and Na to the  $NaC^+Na^-$  salt. This (more than adequate stability condition) is referred to as the stability criterion. We can rewrite the Born-Haber cycle in Figure 4 as follows.



If we substitute the appropriate terms for  $\Delta H_M$  and  $\Delta H_{Na}$  and apply the stability criterion, we have:

$$\begin{aligned} \Delta G_M^O - \Delta G_{Na}^O &= (\Delta H_5^{OM} - \Delta H_5^{ONa}) + (\Delta H_7^{OM} - \Delta H_7^{ONa}) + (\Delta H_8^{OM} - \Delta H_8^{ONa}) \\ &\quad - T(\bar{S}_{MCM}^O - \bar{S}_{NaCNa}^O) - 2T(\bar{S}_M^O - \bar{S}_{Na}^O) \leq 0 \end{aligned} \quad 3.28$$

The term  $(\bar{S}_{MCM}^O - \bar{S}_{NaCNa}^O)$  is the difference in the molar entropies of the salts. This term is not known but it is assumed to be small. All other terms with the exception of  $(\Delta H_5^M - \Delta H_5^{Na})$

are known so that Equation 3.28 can be replaced with the following

$$\Delta H_5^{\text{OM}} - \Delta H_5^{\text{ONa}} \leq -(\Delta H_7^{\text{OM}} - \Delta H_7^{\text{ONa}}) - (\Delta H_8^{\text{OM}} - \Delta H_8^{\text{ONa}}) + 2T[\bar{S}_M^{\text{O}} - \bar{S}_{\text{Na}}^{\text{O}}] \quad 3.29$$

This expression represents the maximum value that  $(\Delta H_5^{\text{OM}} - \Delta H_5^{\text{ONa}})$  can have for the stability criterion to hold. The result of this calculation is shown in Table 5.

Using the same energy cycle that was used to calculate the absolute value of the gas phase enthalpy, we can estimate  $(\Delta H_5^{\text{M}} - \Delta H_5^{\text{Na}})$ . This calculation is much more reliable than the absolute calculation because terms involving sublimation and aqutation of the cryptand cancel out and the use of the Born equation for a difference calculation is more reliable. The result of this cycle is also given in Table 5.

### Discussion

The results of the hypothetical salt calculations are interesting. Of course, the net free energy of the reaction must be greater than zero since we know the alkali elements to be metallic rather than ionic. However, it is evident that not very much stabilization energy is needed to form the anions. Model one, for example, has values which range from  $-3.1 \text{ kcal mol}^{-1}$  for Li to  $+15.3 \text{ kcal mole}^{-1}$  for Cs. This is the most conservative and reasonable estimate of the three

Table 5. Results of the Difference Calculation Using the Stability Criterion.

Metal	$(\Delta H_5^M - \Delta H_5^{\text{Na}})_{\text{max}}$	$(\Delta H_5^M - \Delta H_5^{\text{Na}})_{\text{est}}$
	(kcal mole <sup>-1</sup> )	(kcal mole <sup>-1</sup> )
Li	-12.4	-22.
Na	----	----
K	24.	15.
Rb	25.	21.
Cs	31.8	38.

models, having a larger interatomic distance in the salt compared with model 2 and a lower density than model 3. This serves to illustrate the importance of the radius and structure in determining the stability of a compound. From this it can be argued that the radius of the anion cannot be much smaller than the interatomic distance in the solid minus the metal cation radius as in Equation 3.20. This idea is in accord with the suggestion of Matalon, Golden, and Ottolenghi.<sup>4</sup> They used this assumption, based on ideas of Slater and Pauling, to test the applicability of a charge transfer to the solvent (CTTS) interpretation of  $M^-$  spectra.

The calculations also indicate that if one anion can be found, all the alkali metals should form anions. In particular, there does not seem to be any reason why lithium anions should not form in solution under proper conditions.

The results obtained from the cycle shown in Figure 4 for formation of a salt of the cryptated cation and the alkali anion are not very encouraging. In all cases, the enthalpies are positive. This however, is not too surprising in view of the rough approximations and estimates that were made. Examination of the possible errors in this calculation indicates that the major errors, if corrected, would make the value of  $\Delta H_f$  more negative. For example, the Kapustinskii equation usually gives a value for the lattice energy which is low. This is due to the fact that while the Kapustinskii equation accounts for terms in the lattice energy due to electrostatic interaction, it ignores all contribution due to polarizability

and dispersion energies.

The thermochemical cycle used to calculate  $\Delta H_{\text{gas}}$  is even more in question. The biggest error occurs with the assumption that the non-electrostatic parts of the  $\Delta H_4$  cancel  $\Delta H_2$ . Of the three conformations in which the cryptand can exist, two allow for electron pairs to be oriented toward the solvent. These electron pairs interact very strongly with the solvent (water in these calculations). This would cause the enthalpy of transfer to water from gas for the cryptand to be much more negative than for the non-electrostatic part of the enthalpy of transfer of the cryptate. The cryptate is formed by an ion-dipole interaction of the metal ion with the electron pairs of the complexing agent. Therefore, in the cryptate the electron pairs would be pointing toward the ion, and the solvent would not interact with them. In addition to this are the effects of hydrogen bonding which would be expected to interact differently with the cryptand and cryptate. Fortunately, the error caused by these interactions is expected to remain nearly constant from one ion to the next so that the values that are obtained from this calculation may be used to compare one metal with another. Of course, the value of  $\Delta H_{\text{sub}}$  for the cryptand should be viewed as only a rough estimate. Again, this error is constant regardless of the metal ion used. We might conclude that if one of the alkali metals form a salt of the anion and the cryptated cation then it might be expected that they all would form such a salt.

When the difference in  $\Delta H_f$  for different cryptates are

evaluated, we have a much more reliable calculation. The  $\Delta H_{\text{sub}}$  cancels out and the error in the lattice energy is not severe. The biggest error comes with the use of  $C_{211}$  for lithium. This was used because lithium forms only a very weak complex with  $C_{222}$ , and as a result some of the terms may not cancel out. But, this is assumed to be small. Similar arguments apply to the case in which  $(\Delta H_5^{\text{M}} - \Delta H_5^{\text{Na}})$  was estimated. As mentioned, the terms involving aquation of the cryptand cancel out and the Born equation is more reliable.

From Table 4 it is evident that except for the Cs case,  $(\Delta H_5^{\text{M}} - \Delta H_5^{\text{Na}})_{\text{max}}$  is larger than  $(\Delta H_5^{\text{M}} - \Delta H_5^{\text{Na}})_{\text{est}}$ . This implies that Li, K and Rb form a stable salt as does the sodium cryptate salt of  $\text{Na}^-$ . The fact that this predicts  $\text{CsC}^+\text{Cs}^-$  to be unstable with respect to  $\text{NaC}^+\text{Na}^-$  is not surprising in view of the low complexation constant for  $\text{Cs}^+ + \text{C} \rightarrow \text{CsC}^+$ . The choice of a different cryptand would change this result.

#### Possible Experimental Verification of the Thermodynamic Cycles

With several experiments the values in the thermodynamic cycles described above could be determined much more accurately. In fact, if proper experiments were done, these cycles could be used to determine the value for some of the terms that are difficult to measure. For example, the electron affinity of sodium and the enthalpy of the interaction of the cryptand with the solvent could be evaluated. A summary of needed experiments follows.

1) The enthalpy of sublimation of cryptand could be determined by the Knudsen effusion method. The sublimation used to purify the compound indicates that this could be easily done. A novel modification of the Knudsen method uses the mass spectrometer.<sup>32</sup> This technique utilizes the intensity of the parent peak as a function of temperature to obtain  $\Delta H_{\text{sub}}$ .

2) The enthalpy of the gas phase reaction between the cryptand and the positive sodium ion could be determined by two methods. The most direct and reliable method would be the use of ion cyclotron resonance spectroscopy. The second method is to measure the enthalpy of cryptation in a poor coordination solvent and use a thermochemical cycle to find the heat of the gas reaction. In the poor coordination solvent, hydrogen bonding and the electron pair interaction with the solvent would be much smaller than in water.

3) The enthalpy and free energy of the sodium cryptate solid could be determined by the following set of thermochemical studies.

(a) Enthalpy of solution  $[\text{NaCNa}_{(s)} \rightarrow \text{NaC}^+_{(\text{solv.})} + \text{Na}^-_{(\text{solv.})}]$  in an amine or ether.

(b) The enthalpy for the complexation reaction  $[\text{Na}_{(s)} + \text{C}_{(s)} \rightarrow \text{NaC}^+_{(\text{solv.})} + \text{Na}^-_{(\text{solv.})}]$  in the same amine or ether.

(c) The third law entropy for  $\text{NaC}^+\text{Na}^-_{(s)}$  and for  $\text{C}_{(s)}$ .

All of these studies would involve a great deal of experimental work and time because of the reactivity of the reducing species and the care necessary in handling the solution.



CHAPTER 4  
NMR EXCHANGE STUDIES OF ALKALI METAL  
ANION SOLUTIONS

### Rationale

The impetus for this study came from the work of Dye and Ceraso, in which the NMR spectrum of  $\text{Na}^+$  was observed.<sup>15</sup> It was felt that the use of a different complexing agent would yield new and different information about the nature of the anion interactions in solution. Although  $\text{C}_{222}$  had been used for the original work, 18-crown-6 (18-C-6) was tried for several reasons. First, solution studies showed that 18-C-6 increased the solubility of sodium in methylamine (MA) to more than .35M which is high enough to give good NMR spectra. In addition this system can form unusual solid complexes.<sup>33</sup> Secondly, 18-C-6 is commercially available and is much lower in price than  $\text{C}_{222}$ . Figure 5 shows a comparison of the  $^{23}\text{Na}$  NMR spectrum of a solution of  $\text{C}_{222}$  and Na in MA with that obtained with 18-C-6 and Na in MA at nearly the same temperature. It is evident from these spectra that the 18-C-6 system is affected by exchange broadening. This exchange broadening is reasonable since it is known that with salt solutions the crown exchange rates are faster<sup>34</sup> than cryptate exchange rates.<sup>35</sup> This immediately suggests that a detailed study of the temperature dependence of the NMR spectra of solutions which contain both the 18-C-6 complex and  $\text{Na}^+$  would yield information about exchange processes. Figure 6 shows the changes which occur in the  $^{23}\text{Na}$  NMR spectra of the  $\text{Na}^+$ ,  $\text{NaC}^+$  system (with C=18-C-6) as a function of temperature. Fortunately, the

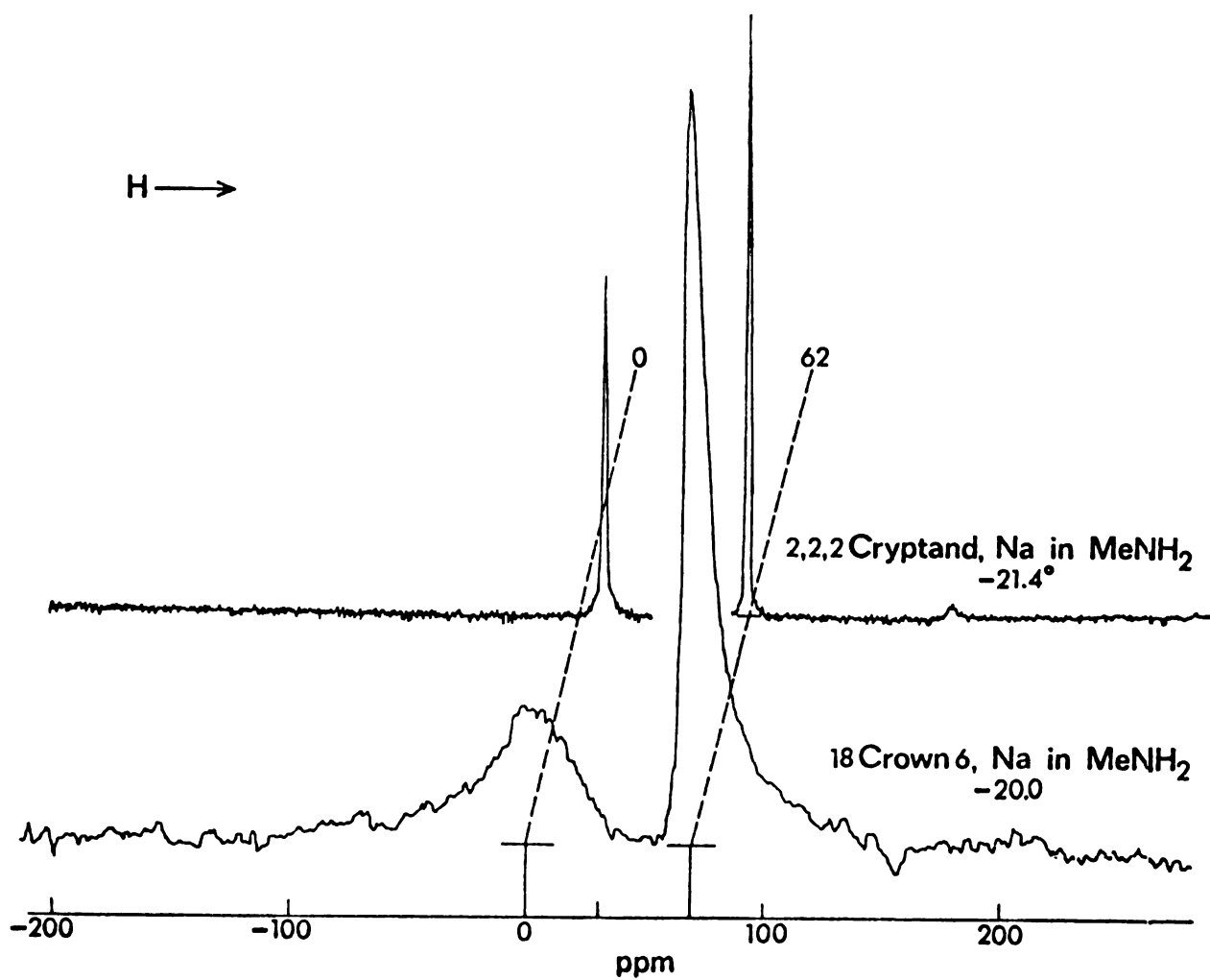


Figure 5.  $^{23}\text{Na}$  NMR Spectra of  $\text{Na}^+\text{C}_{222}$  and  $\text{Na}^+$  (18-C-6),  $\text{Na}^+$  in Methyamine.

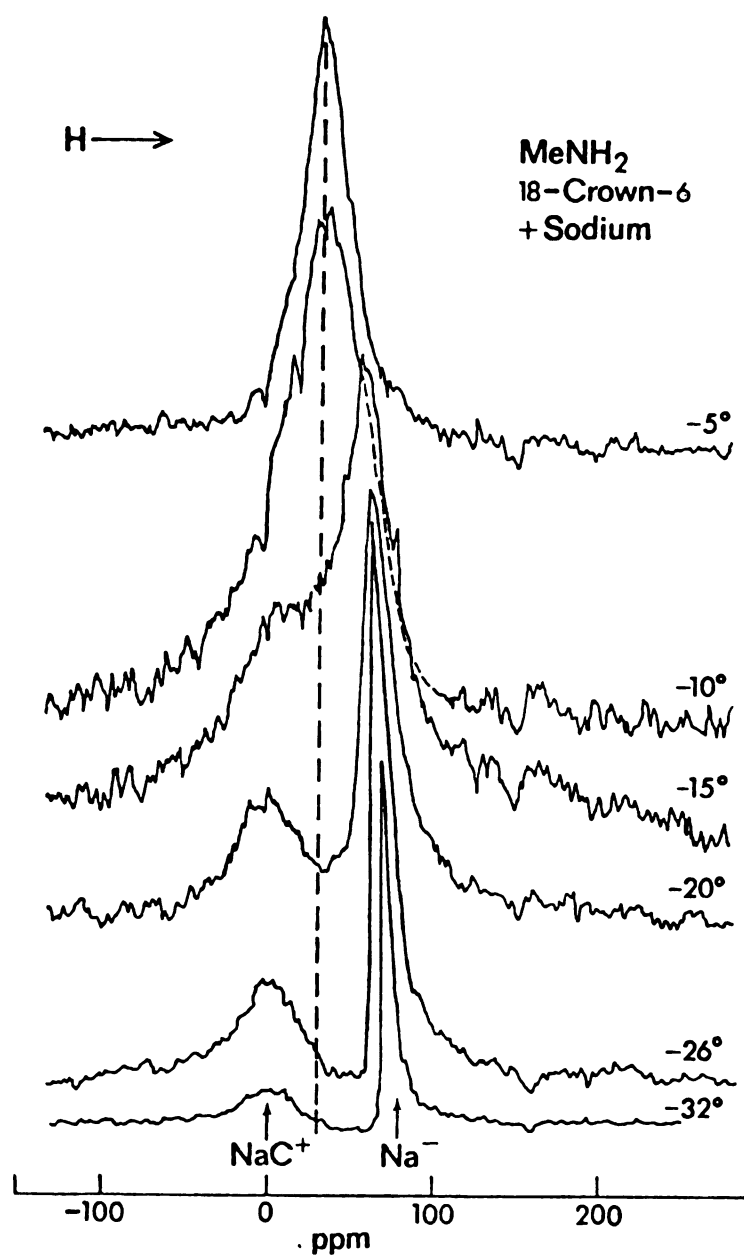


Figure 6.  $^{23}\text{Na}$  NMR Spectra of  $\text{Na}^+$  (18-C-6),  $\text{Na}^-$  in Methylamine at Various Temperatures.

coalescence temperature (-10 to 0°C) is low enough to avoid rapid decomposition of these reactive solutions. A study of this exchange process might yield two types of information. Since the relaxation time is given by

$$\frac{1}{\tau_i} = \frac{\text{Rate of leaving site } i}{\text{Concentration of species in site } i} \quad 4.1$$

a study of the concentration dependence of the relaxation time could yield the mechanism by which the exchange is occurring. From the mechanism the rate of exchange of electrons between the anion and the cation might be measured.

### Three Site Exchange Processes

The anion exchange system differs from the previous crown and cryptate systems studied in that three sites are available for the nucleus. The sites are  $\text{Na}^+$  (site A),  $\text{NaC}^+$  (site B) and  $\text{Na}^-$  (site C). (It is even possible that a fourth site, the sodium monomer, might be important). The modified Bloch equations for the three site case are similar to the two site equations and are given as follows.

$$-[\alpha_A + \frac{1}{\tau_A}]G_A + \frac{1}{\tau_{BA}}G_B + \frac{1}{\tau_{CA}}G_C = i\gamma H_1 M_O^P A \quad 4.2$$

$$-[\alpha_B + \frac{1}{\tau_B}]G_B + \frac{1}{\tau_{AB}}G_A + \frac{1}{\tau_{CB}}G_C = i\gamma H_1 M_O^P B \quad 4.3$$

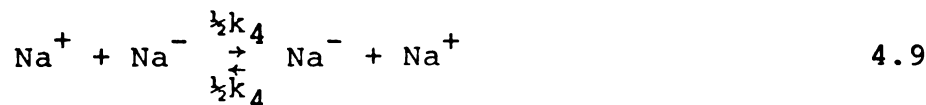
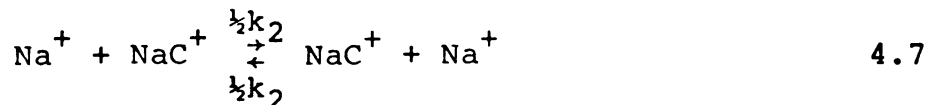
$$-[\alpha_C + \frac{1}{\tau_C}]G_C + \frac{1}{\tau_{AC}}G_A + \frac{1}{\tau_{BC}}G_B = i\gamma H_1 M_O^P C \quad 4.4$$

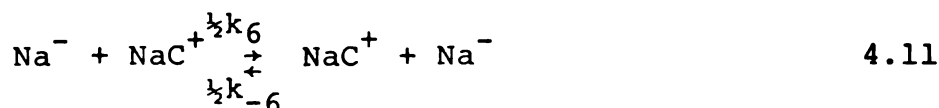
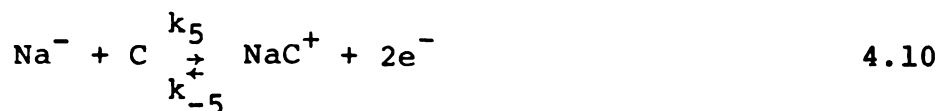
The terms have the same meaning as in the two site case except for the terms involving  $\tau$ . For a nucleus at any given site there exist two other sites to which it can jump. For example,  $\frac{1}{\tau_{AB}}$  = average lifetime in position A before the nucleus jumps to position B.  $\tau_{AC}$ ,  $\tau_{BA}$ ,  $\tau_{BC}$ ,  $\tau_{CA}$  and  $\tau_{CB}$  are similarly defined. In addition a term  $\frac{1}{\tau_A}$  can be defined as

$$\frac{1}{\tau_A} = \frac{1}{\tau_{AB}} + \frac{1}{\tau_{AC}} \quad 4.5$$

so that  $\frac{1}{\tau_A}$  is the average lifetime in site A before a jump to either site B or site C. The definition of  $\frac{1}{\tau_B}$  and  $\frac{1}{\tau_C}$  are similar.

Dr. Dye has suggested several possible mechanisms to describe the process of exchange in the  $\text{Na}^-$  system. These are:





By using mass and charge balance considerations it is not difficult to relate the mean lifetime of a nucleus in any site to the rate constants and the concentrations of the various species. When this is done with the six exchange mechanisms (4.6-4.11) the following expressions are obtained for :

$$\frac{1}{\tau_A} = k_{-1}[\text{C}] + k_2[\text{NaC}^+] + k_{-3}[\text{e}^-]^2 + k_4(\text{Na}^-) \quad 4.12$$

or

$$\begin{aligned} \frac{1}{\tau_A} = & (\text{NaC}^+)^2 \left(1 - \frac{P_C}{P_B}\right)^2 \left[\frac{k_{-1}k_{-5}P_B}{k_5P_C} + k_{-3}\right] + k_2[\text{NaC}^+] \\ & + k_4 \frac{P_C}{P_B}[\text{NaC}^+] \end{aligned} \quad 4.13$$

$$\frac{1}{\tau_B} = k_1 + k_2[\text{Na}^+] + k_{-5}[\text{NaC}^+]^2 \left(1 - \frac{P_C}{P_B}\right)^2 + k_6 \frac{P_C}{P_B}(\text{NaC}^+) \quad 4.14$$

and

$$\begin{aligned} \frac{1}{\tau_C} = & k_3 + \frac{k_3k_4 P_C}{k_{-3} P_B (\text{NaC}^+) \left(1 - \frac{P_C}{P_B}\right)^2} + \\ & + k_{-5} \frac{P_B}{P_C}(\text{NaC}^+)^2 \left(1 - \frac{P_C}{P_B}\right)^2 + k_6(\text{NaC}^+) \end{aligned} \quad 4.15$$

These expressions provide a powerful probe for determining the mechanism which dominates the exchange of the 18-C-6 system. From measurements on the salt and crown system without  $\text{Na}^-$  present, mechanism 4.6 can be distinguished from mechanism 4.7 because of the dependence of  $\frac{1}{\tau_B}$  on the  $\text{Na}^+$  concentration. Mechanism 4.10 can be distinguished from mechanism 4.11 by the dependence of  $\frac{1}{\tau_B}$  on  $\text{NaC}^+$  concentration. The relative concentrations of  $\text{NaC}^+$  and  $\text{Na}^-$  can be changed by adding  $\text{NaI}$  to the crown before the solution is placed on the metal mirror. This produces a system which contains  $\text{NaC}^+$ ,  $\text{Na}^-$  and  $\text{I}^-$  provided decomposition is not severe.

#### Reduction of the Three-site Equations to Two-site Equations

Although there are three possible sites for the sodium nucleus only two sites can be detected as a result of the large complexation constant of the crown. It would be easy to assume that because the concentration of the third site is very small this case reduces automatically to a two site system. This however is not always the case. Since the relative concentration of a site is related to the mean lifetime of a species in that site, when  $p_A$  is small,  $\tau_A$  may also be small and terms involving  $p_A$  can make a significant contribution to the exchange time through the ratio  $\frac{p_A}{\tau_A}$ . For the case in which  $p_A$  is very small the right-hand side of equation 4.2 becomes negligible and, as suggested by



Dye, we can solve for  $G_A$ . We then have

$$G_A = \frac{1}{\tau_{BA}[\alpha_A + \frac{1}{\tau_A}]} \cdot G_B + \frac{1}{\tau_{CA}[\alpha_A + \frac{1}{\tau_A}]} G_C \quad 4.16$$

If we assume that the contribution of  $\alpha_A$  is very small compared with  $\frac{1}{\tau_A}$  we then have

$$G_A = \frac{\tau_A}{\tau_{BA}} G_B + \frac{\tau_A}{\tau_{CA}} G_C \quad 4.17$$

The neglect of  $\alpha_A$  is reasonable except when the lines are very broad in the absence of exchange. Only when  $\tau_A$  becomes very small or the line in question is very broad will a site of very low concentration affect the spectrum. Substituting Equation 4.17 into 4.3 and 4.4 gives the following:

$$-\left[\alpha_B + \frac{1}{\tau_B} - \frac{\tau_A}{\tau_{AB}\tau_{BA}}\right]G_B + \frac{1}{\tau_{CB}}\left[\frac{\tau_A}{\tau_{AB}\tau_{CA}}\right]G_C = i\gamma H_1 M_O P_B \quad 4.18$$

$$-\left[\alpha_C + \frac{1}{\tau_C} - \frac{\tau_A}{\tau_{AC}\tau_{CA}}\right]G_C + \left[\frac{1}{\tau_{BC}} + \frac{\tau_A}{\tau_{AC}\tau_{BA}}\right]G_B = i\gamma H_1 M_O P_C \quad 4.19$$

It can be shown that the coefficient of  $G_B$  in Equation 4.18 is equal to the coefficient of  $G_A$  in 4.19 and the same is true with the coefficients of  $G_C$ . Therefore we can rewrite these two equations as follows:

$$-\left[\alpha_B + \frac{1}{\tau'_B}\right]G_B + \frac{1}{\tau'_C} G_C = i\gamma H_1 M_O P_B \quad 4.20$$

$$-\left[\alpha_C + \frac{1}{\tau'_C}\right]G_C + \frac{1}{\tau'_B} G_B = i\gamma H_1 M_O P_C \quad 4.21$$

where

$$\frac{1}{\tau'_B} = \frac{1}{\tau_{BC}} + \frac{1}{\tau_{BA}} \left(1 + \frac{\tau_{AC}}{\tau_{AB}}\right) \quad 4.22$$

and

$$\frac{1}{\tau'_C} = \frac{1}{\tau_{CB}} + \frac{1}{\tau_{CA}} \left(1 + \frac{\tau_{AB}}{\tau_{AC}}\right) \quad 4.23$$

Since Equations 4.20 and 4.21 are identical in form to the two-site Bloch equations, we can use the solutions for the two site case to deal with a three-site case provided the concentration of one of the sites is very low and provided also that this site is not paramagnetic (which would give a large value of  $\alpha$ ). Once  $\tau'_B$  and  $\tau'_C$  have been obtained from a fit of the line shapes, they can be related to a mechanism. For example, if the exchange occurred via mechanisms 4.6 and 4.8,  $\frac{1}{\tau'_B}$  would be related to the concentrations and the rate constants as follows:

$$\frac{1}{\tau'_B} = \frac{k_1}{\left[1 + \frac{k_1 P_B}{k_3 P_C}\right]} \quad 4.24$$

and

$$\frac{1}{\tau'_C} = \frac{k_3}{\left[1 + \frac{k_3 P_C}{k_1 P_B}\right]} \quad 4.25$$

Table 6 lists several mechanisms and their expressions

Table 6. Possible Exchange Mechanisms and Expressions for  $1/\tau_B'$ .

Mechanism through which $\text{Na}^-$ to $\text{NaC}^+$ exchange occurs	Expression for $\frac{1}{\tau_B'}$
<p>Mech. A</p> $\text{NaC}^+ \xrightleftharpoons[k_{-1}]{k_1} \text{Na}^+ + \text{C}$ $\text{Na}^- \xrightleftharpoons[k_{-3}]{k_3} \text{Na}^+ + 2\text{e}^-$	$\frac{1}{\tau_B'} = \frac{k_1}{\left[1 + \frac{k_1 P_B}{k_3 P_C}\right]}$
<p>Mech. B</p> $\text{NaC}^+ \xrightleftharpoons[k_{-1}]{k_1} \text{Na}^+ + \text{C}$ $\text{Na}^+ + \text{Na}^- \xrightleftharpoons[k_4]{k_4} \text{Na}^- + \text{Na}^+$	$\frac{1}{\tau_B'} = \frac{k_1}{\left[1 + \frac{k_{-1} (C_T - (\text{NaC}^+))}{2k_4 (\text{Na}^-)}\right]}$
<p>Mech. C</p> $\text{Na}^- + \text{NaC}^+ \xrightleftharpoons[k_6]{k_6} \text{NaC}^+ + \text{Na}^-$	$\frac{1}{\tau_B'} = 2k_6 (\text{Na}^-)$
<p>Mech. D</p> $\text{Na}^- + \text{C} \xrightleftharpoons[k_{-5}]{k_5} \text{NaC}^+ + 2\text{e}^-$	$\frac{1}{\tau_B'} = \frac{k_{-5}}{\left[\frac{(C_T - \text{NaC}^+) K_5 P_C}{P_B}\right]}$

for  $\tau_B$ . These expressions allow the different exchange mechanisms to be tested by the concentration and relative population dependence on  $\tau_B$  of the species  $\text{Na}^-$ ,  $\text{NaC}^+$ ,  $\text{e}^-$  and C.

### Information From Non-exchanging Systems

In the process of independently measuring  $\omega_A$ ,  $T_{2A}$ ,  $\omega_B$  and  $T_{2B}$ , other information can be extracted from the non-exchanging system. One such piece of information is the activation energy for molecular reorientation of solvent molecules close to the ion. In general if a simple activation process is assumed, then

$$\tau_C = A \exp (-E_r/RT) \quad 4.26$$

Where A is a constant and  $\tau_C$  is the correlation time.<sup>36</sup> Furthermore, if the quadrupole coupling constant and the field gradient are insensitive to temperature changes then

$$T_2^{-1} \propto \tau_C = A' \exp (E_r/RT) \quad 4.27$$

The activation energy,  $E_r$ , is the slope of a plot of the log of the line width ( $T_2^{-1}$ ) versus reciprocal temperature. The agreement between this method and other methods for determining  $E_r$  is good.<sup>36</sup>

The values of  $T_{2A}$ ,  $T_{2B}$ ,  $\omega_A$  and  $\omega_B$  are given in Table 7.

Table 7. The Variation of the Linewidth and Chemical Shift of the Free and Complexed  $^{23}\text{Na}$  Cation with Temperature.

Temp ( $^{\circ}\text{C}$ )	$\Delta\nu_{1/2}$ (Hz) <sup>1</sup>	$T_2$ (msec) <sup>2</sup>	$\Delta\text{ppm}$ <sup>3,4</sup>
Free Cation			
12.4	7.0	45.4	-9.4
5.7	6.9	45.8	-9.3
+ 0.7	7.6	42.1	-9.2
- 6.7	8.1	39.5	-9.3
-11.0	8.4	37.9	-9.3
-17.8	9.6	33.2	-9.3
-23.9	10.6	30.1	-9.3
-32.8	12.3	25.8	-9.3
-41.6	15.4	20.7	-9.3
Complexed Cation			
10.7	244.9	1.30	5.6
- 2.5	320.3	1.00	6.0
-13.5	391.5	0.81	5.6
-20.0	481.7	0.66	6.3
-29.0	656.3	0.50	8.6

<sup>1</sup>For all tables, full-width at half-height in Hertz corrected for field in homogeneity.

<sup>2</sup> $\pm 0.5$  msec for free cation and  $\pm 0.03$  msec for complexed cation.

<sup>3</sup>For all tables, relative to aqueous  $\text{Na}^+$  at infinite dilution (actual reference solution was saturated aqueous  $\text{NaCl}$ ).

<sup>4</sup> $\pm 0.4$  ppm.

The plots of  $\log T_2^{-1}$  vs. reciprocal temperature are presented in Figure 7. A plot of  $\log \eta$  vs. reciprocal temperature for pure MA is also included in Figure 7. The values for the activation energy,  $E_r$ , for the free and complexed NaI are

$$E_r \text{ for } \approx .15 \text{ MNaI} = \underline{1.8 \pm .1} \text{ kcal mole}^{-1}$$

$$E_r \text{ for } \approx .15 \text{ MNaC}^+\text{I}^- = \underline{3.2 \pm .2} \text{ kcal mole}^{-1}$$

$T_{2C}$  and  $\omega_C$  (line width and Larmor frequency of  $\text{Na}^+$ ) were obtained from the  $C_{222}$  Na and MA system which is in the slow exchange limit from  $-40^\circ$  to  $0^\circ\text{C}$ . The line width of  $\text{Na}^+$  changed only 2Hz over the entire region (12.5-14.5 Hz). The average value of this was obtained and corrected for inhomogeneous broadening. The average value was used for  $T_{2C}$ .

#### 18-C-6 Salt Exchange System

The work on the sodium salt exchange with 18-C-6 proved to be very difficult. Sodium iodide was chosen for the salt because its solubility appeared to be higher than that of either  $\text{NaBo}_4$  or  $\text{NaSCN}$ . Even with NaI, precipitation occurred in a .1 M solution at about  $-40^\circ\text{C}$ . At this temperature the system was in the rapid exchange region. Typical results for the linewidth and chemical shift are shown in Table 8. It is unfortunate that the exchange is

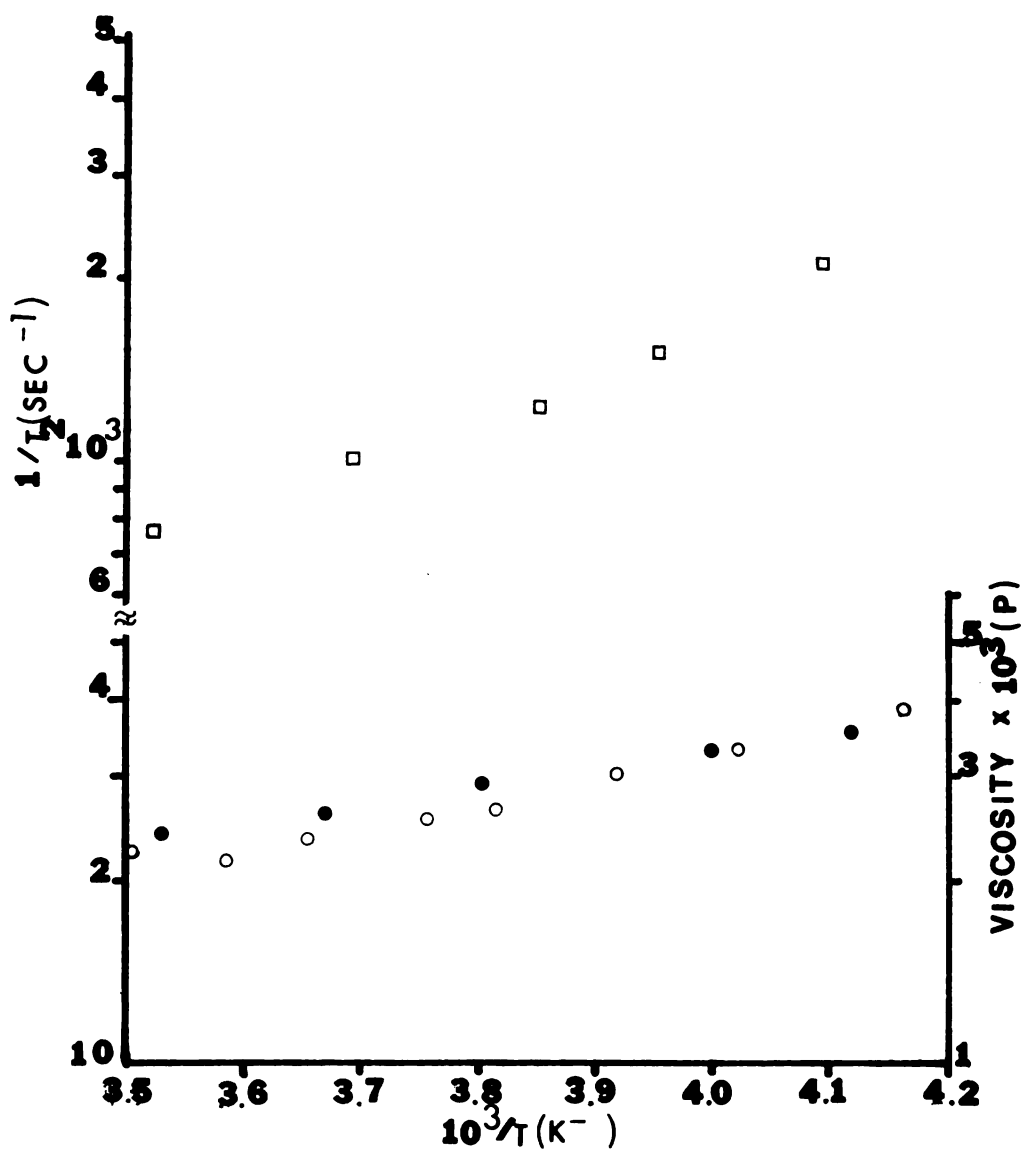


Figure 7. Semilog Plot of Transverse Relaxation Times vs Reciprocal Temperature for Free NaI (○) and a 1:1 Complex of NaI and 18-C-6 (□). The log of the Viscosity of Methylamine is Plotted for Comparison (●).

Table 8. The Variation of the Chemical Shifts,  $\Delta$ , and the Transverse Relaxation Times,  $T_2$  for 18-C-6, NaI Exchanging System. Concentrations of Complexed and Free Sodium Ions are Equal.

Temp ( $^{\circ}\text{C}$ )	$\Delta$ ppm	$\Delta\nu_{\frac{1}{2}}$ (Hz)	$T_2$ (msec)
0.0	-1.6	191.3	1.7
-15.0	-1.8	254.8	1.3
-19.8	-2.2	341.5	.93
-30.4	-1.6	403.0	.79



so fast since it is important to distinguish between mechanisms 4.6 and 4.7 for the release of  $\text{Na}^+$  from the complex. It is fair to assume however that this exchange occurs via mechanism 4.6 based on previous studies on the crowns and cryptates.<sup>34,37</sup>

### Results of $\text{Na}^+$ , 18-C-6 Exchange Studies

Three types of  $\text{Na}^+$  solutions can be made for study. The first is a solution in which the populations of  $\text{Na}^+$  and  $\text{NaC}^+$  are equal ( $P_B = P_C$ ). This type of solution can be studied at different absolute concentrations. The second type of solution is one in which a non-reducible salt is added (NaI) along with an equimolar amount of 18-C-6. This has the effect of making  $P_B > P_C$  which allows the effect due to the relative populations to be quantitatively studied. The third type of solution which can be readily prepared contains 18-C-6 in excess. By using solutions of these three compositions a severe test can be made of the mechanisms previously discussed.

Five samples were prepared for rigorous data analysis. The nature of these solutions is listed in Table 9. The lineshapes of these five samples were fit as described. A few representative line printer plots from program KINFIT are present in Figures 8 and 9. In the figures x corresponds to the input data, o corresponds to the calculated value and = to the points in which the calculated value is equal

Table 9. Composition of Samples Used for Line Shape Fitting.

Sample	$[\text{NaC}^+]$	$[\text{Na}^-]$	
	Mole liter <sup>-1</sup>	Mole liter	
1	.1	.1	
2	.17	.12	NaI Added
3	.17	.17	
4 <sup>1</sup>	.15	.15	Excess Crown Added
5	.19	.1	NaI Added

<sup>1</sup>Relative populations determined by allowing the computer to adjust a sixth parameter ( $P_A$ ).

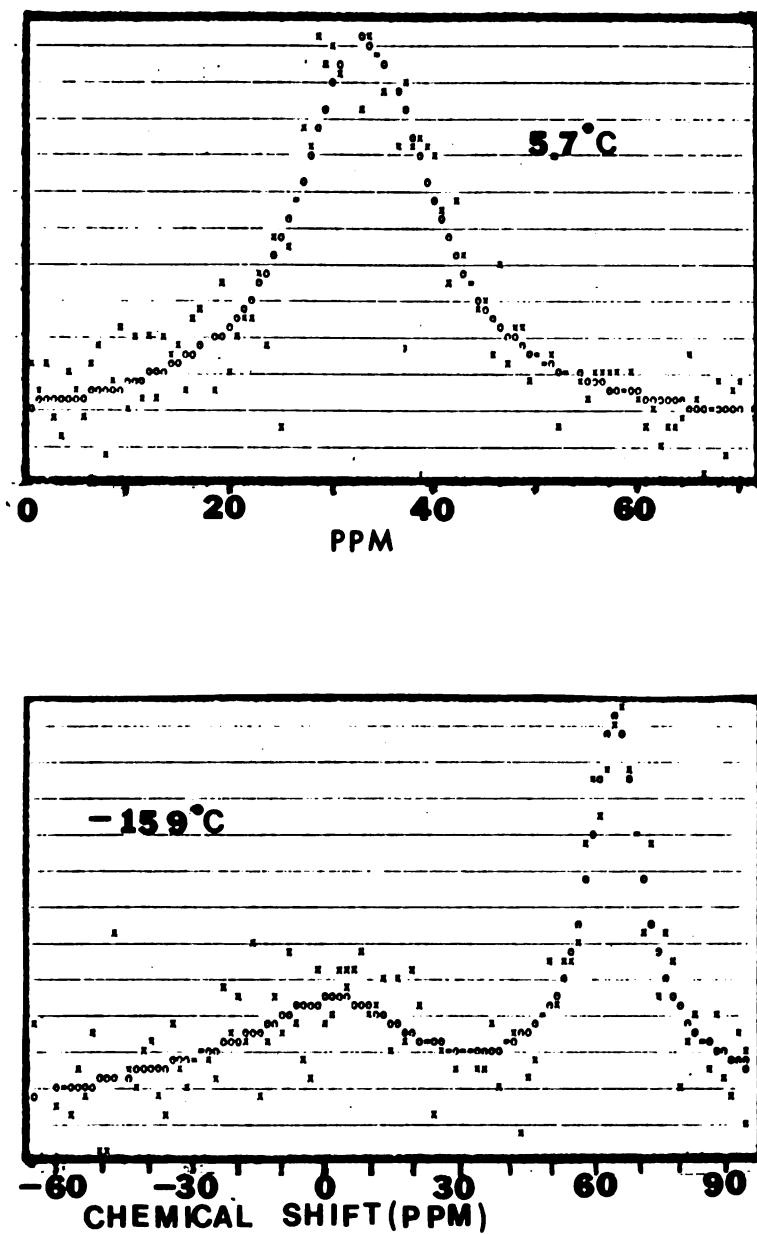


Figure 8. Line Printer Plot of Sample 1 at  $+5.7^{\circ}\text{C}$  and  $-15.9^{\circ}\text{C}$ .

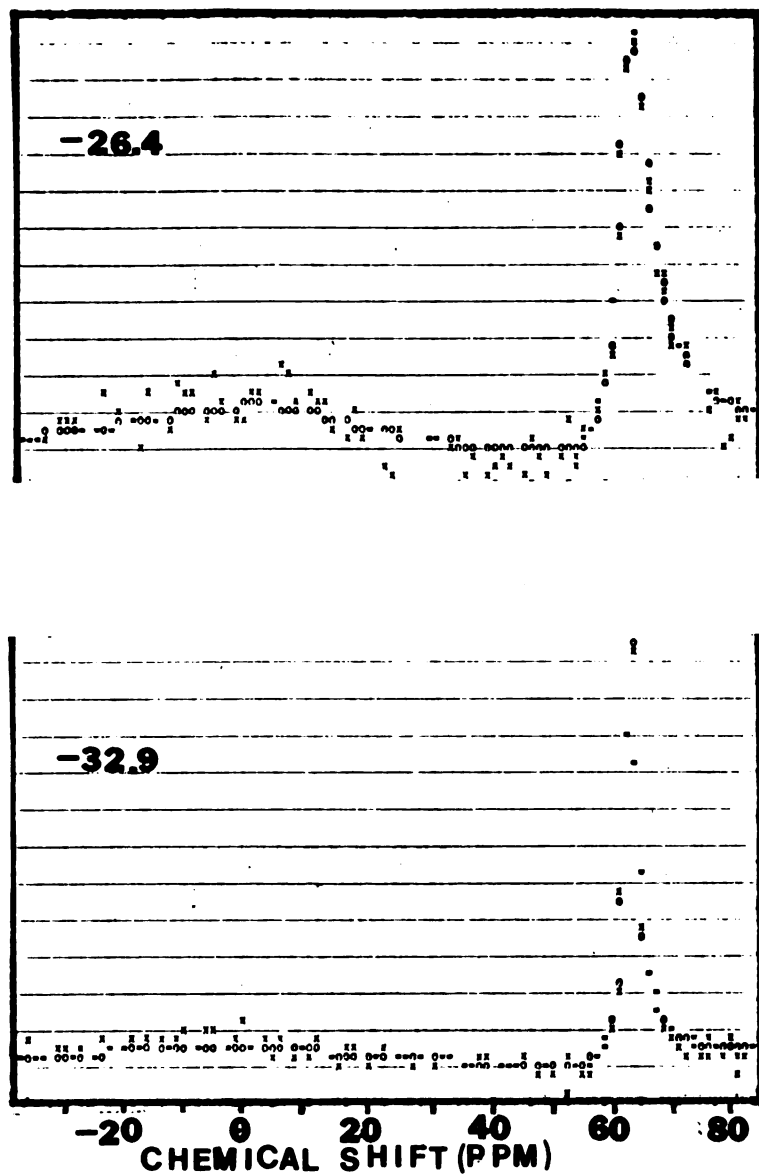


Figure 9. Line Printer Plot of Sample 1 at  $-26.4^{\circ}\text{C}$  and  $-32.9^{\circ}\text{C}$ .

to the actual data within lineprinter resolution. The values of  $\tau$ , reciprocal temperature and  $\frac{1}{\tau_B}$  for the samples are listed in Tables 10-14. The apparent activation energy ( $E_a$ ) can be obtained by fitting the data with the equation  $\frac{1}{\tau_B} = Ae^{-E_a/T}$ . These data are plotted for the samples in Figure 10 and the results are tabulated in Table 15.

### Uses of Other Complexing Agents

The great variety of complexing agents available offers unlimited opportunity for studying alkali metal NMR. One system in which preliminary results have been obtained is 15-C-5, sodium and MA. Unlike the 18-C-6 complexing agent the 15-C-5 compound gives a relatively narrow NMR line. Values of the linewidth and chemical shift for 1:1 and 3:1 ratio of [NaI] to [15-C-5] solutions are tabulated in Table 16. The 3:1 solution is in the rapid exchange limit even at  $-40^\circ\text{C}$  as was the case with the 18-C-6 system. The 15-C-5 was used to prepare a sample containing  $\text{Na}^-$ . The sample gave a very weak  $\text{Na}^-$  peak in the NMR which coalesced with the  $\text{NaC}^+$  peak at approximately  $33.0^\circ\text{C}$ . Several spectra are shown in Figure 11. Other data are presented in Table 17. The reason for the small intensity of the  $\text{Na}^-$  peak in the 15-C-5 system may be due to the presence of solvated electrons or to solution decomposition. If solvated electrons are present then the crown would be present in excess and the concentration of the anion would not be as high

Table 10. The Temperature Dependence of the Exchange Time  $\tau$  and  $1/\tau_B$  for Sample 1.

Temp <sup>-1</sup> (10 <sup>3</sup> K <sup>-1</sup> )	$\tau$ (secx10 <sup>3</sup> )	$\frac{1}{\tau_B} \times 10^{-3}$	$\sigma \frac{1}{\tau_B}^a$
3.586	.04409	11.34	1946.9
3.658	.08733	5.725	747.0
3.731	.1703	2.936	610.0
3.800	.3151	1.587	127.0
3.887	.7676	.651	60.0
3.974	1.678	.298	25.0
4.012	1.998	.250	12.0
4.119	5.389	.0928	3.9

<sup>a</sup>For all tables  $\sigma \frac{1}{\tau_B}$  is linear estimate of the standard deviation of  $\frac{1}{\tau_B}$ .

Table 11. The Temperature Dependence of the Exchange Time  $\tau$  and  $1/\tau_B$  for Sample 2.

$\text{Temp}^{-1} (10^3 \text{K}^{-1})$	$\tau (\text{sec} \times 10^3)$	$\frac{1}{\tau_B} \times 10^{-3}$	$\sigma \frac{1}{\tau_B}$
3.571	0.05766	4.960	700.0
3.629	0.1398	2.046	200.0
3.719	0.3477	0.822	55.0
3.803	0.9352	0.3058	32.0
3.889	1.840	0.1554	13.0
3.950	2.899	0.987	6.5
4.054	8.588	0.0333	3.5
4.178	30.19	0.009	0.4
4.296	314.88	.000909	0.3

Table 12. The Temperature Dependence of the Exchange Time  $\tau$  and  $1/\tau_B$  for Sample 3.

$\text{Temp}^{-1} (10^3 \text{K}^{-1})$	$\sigma_{K-1}^1 \times 10^3$	$\tau (\text{sec} \times 10^3)$	$\frac{1}{\tau_B} \times 10^{-3}$	$\sigma \frac{1}{\tau_B}$
3.518	.0248	.04344	11.51	900.
3.610	.026	.08899	5.619	470.
3.684	.0271	.1444	3.463	440.
3.773	.0285	.4780	1.046	64.
3.883	.0301	1.723	0.3283	20.
3.979	.0316	4.767	.1049	4.
4.106	.0337	21.9	.02282	.6

<sup>1</sup> Estimate of Standard Deviation in  $\text{Temp}^{-1}$ .



Table 13. The Temperature Dependence of the Exchange Time  $\tau$  and  $1/\tau_B$  for Sample 4.

$\text{Temp}^{-1} (10^3 \text{K}^{-1})$	$(\text{sec} \times 10^3)$	$\frac{1}{\tau_B} \times 10^{-2}$	$\sigma \frac{1}{\tau_B} \times 10^{-2}$
3.607	.09523	49.3	5.3
3.668	.1663	28.3	2.3
3.732	.4493	10.46	.48
3.793	.8769	5.36	.37
3.8424	1.731	2.71	.16
3.9085	4.505	1.04	.03
3.9896	9.129	.51	.01

Table 14. The Temperature Dependence of the Exchange Time  $\tau$  and  $1/\tau_B$  for sample 5.

Temp ( $10^3 K^{-1}$ )	(sec $\times 10^3$ )	$\frac{1}{\tau_B} \times 10^{-2}$	$\sigma \frac{1}{\tau_B} \times 10^{-2}$
3.569	.1914	10.0	.80
3.661	.3688	5.2	.7
3.770	1.383	1.388	.218
3.842	3.946	.48	.08
3.982	10.56	.18	.01
4.243	80.26	.0239	.0036

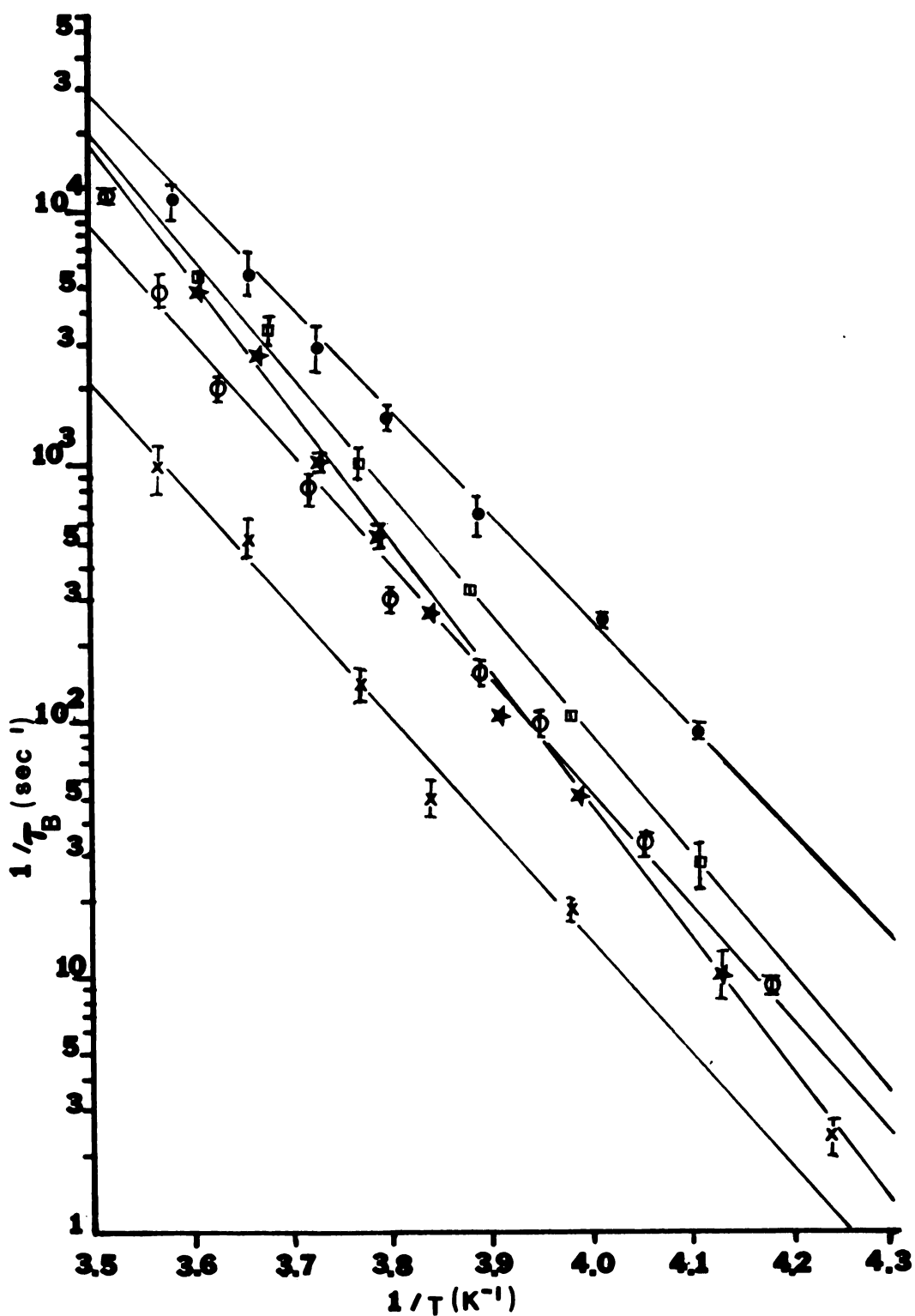


Figure 10. Arrhenius Plots of  $1/\tau_B$  vs Reciprocal Temperature for Sample 1 (●), Sample 2 (○), Sample 3 (□), Sample 4 (★), and Sample 5 (x).

Table 15. Apparent Activation Energy and  $1/\tau_B$  (0°C) for Alkali Anion to Complexed Cation Exchanging Systems.

Sample #	$E_a^a$ (kcal mole <sup>-1</sup> )	$\frac{1}{\tau_B}^a$ (0°C) x 10 <sup>-3</sup>
1	18.2± .3	5.6±.2
2	20.7± .7	1.7±.2
3	21.2± .9	3.3±.3
4	25.2±1.2	2.6±.3
5	19.0± .1	4.2±.5

<sup>a</sup>Deviations listed are linear estimates of the standard deviations obtained with program KINFIT.

Table 16. The Variation of the Linewidth and Chemical Shift With Temperature for Two Solutions Which Contain the 15-C-5 Complexing Agent and NaI.

Temp	$\Delta \nu_{\frac{1}{2}}$	$T_2$ (msec)	$\Delta$ ppm
1:1 Ratio of $\text{Na}^+$ to Crown			
+ 2.5	24.4	13.0	-3.1
- 9.7	34.2	9.3	-2.8
-17.4	39.0	8.2	-2.8
-26.2	53.7	5.9	-2.8
-38.3	73.2	4.3	-2.6
3:1 Ratio of $\text{Na}^+$ to Crown			
1.4	29.3	10.9	-9.3
- 9.0	29.3	10.9	-8.1
-22.3	43.9	7.2	-6.8
-34.3	63.5	5.0	-4.7
-41.8	87.9	3.6	-3.5

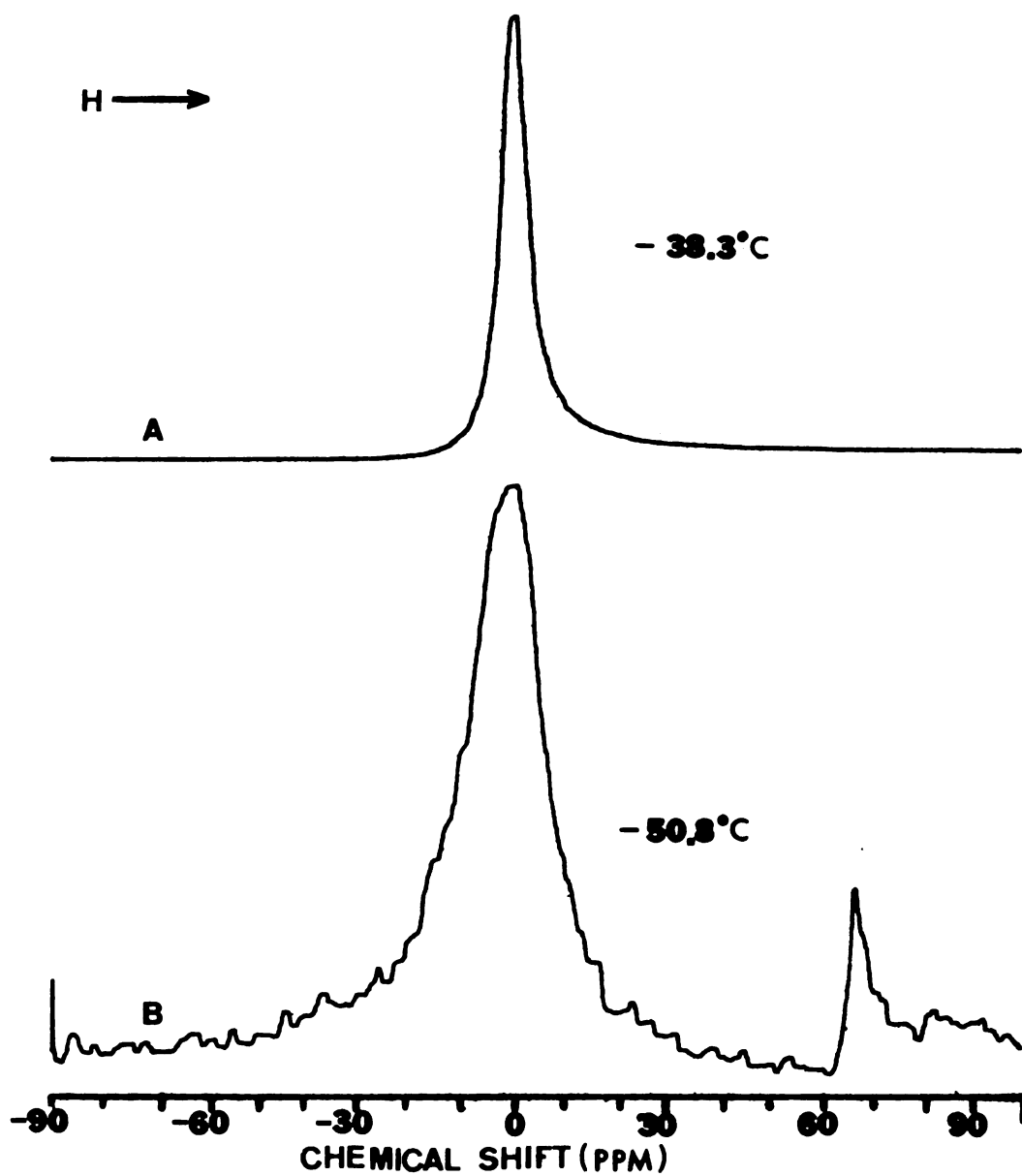


Figure 11.  $^{23}\text{Na}$  NMR Spectra of: A. Equimolar NaI and 15-C-5 in Methylamine B. 15-C-5, Na in Methylamine.

Table 17. The Variation of the Linewidth and Chemical Shift of  $\text{NaC}^+$  and the Chemical Shift of  $\text{Na}^-$  with Temperature for the 15-C-5 System in Methylamine.

Temp ( $^{\circ}\text{C}$ )	$\nu_{\frac{1}{2}}$ $\text{NaC}^+$	$\Delta\text{ppm NaC}^+$	$\Delta\text{ppm Na}^-$	$\frac{1}{\tau_B}$ ( $\text{msec}^{-1}$ ) <sup>1</sup>
-28.8	175.8	-1.85	----	3.4
-39.8	190.4	-1.85	64.9	2.7
-45.1	233.5	0.0	65.8	2.1
-50.8	243.3	0.0	64.3	2.0
-56.0	268.6	-3.0	63.7	1.80

<sup>1</sup>Estimate from spectra  $\pm 20\%$ .

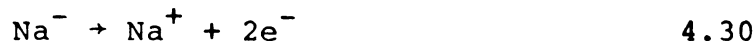
as in the 18-C-6 case. More work is needed to characterize the 15-C-5 crown exchange. However, it appears that this will be an interesting system to study.

### Discussion of Results

For the systems in the absence of exchange, the results are reasonable. From the work of Popov<sup>38</sup> in which the donor number of basic solvents was correlated with the sodium chemical shift it is expected that the chemical shift of  $\text{Na}^+$  in MA would be near that in ethylamine (-11.3) and ammonia (-13.1). The chemical shift for the salt in MA was not extrapolated to infinite dilution so the results are not exactly comparable. However, the results given in Table 7 are in good agreement with expectation.

The results of the  $\text{Na}^+$  systems which show exchange are very interesting. Several facts are evident from the data presented previously. First, the apparent activation energy ( $E_a$ ) is very high ranging from 18.2 - 25.2 kcal mole<sup>-1</sup>. This is in sharp contrast to the results of Shchori et al.<sup>34</sup> who found that the dibenzo-18-crown-6 activation energy for cation exchange was relatively low (8.3 kcal mole<sup>-1</sup>) and independent of solvent. Studies in this laboratory of the decomplexation of  $\text{C}_{222}$  give activation energies in the range of 12-16 kcal mole<sup>-1</sup> depending upon the solvent. It also appears that when 18-C-6 is added to a solution containing  $\text{Na}^+$  the reaction





does not proceed to a great extent. This was determined by allowing the computer to adjust  $P_C$  and  $P_B$  for a sample in which 18-C-6 was added after the solution had been prepared. The activation energy also appears to be extremely sensitive to the presence of free crown. In view of this it is clear that  $\frac{1}{\tau_B}$  is very dependent on the concentration of various species in the sample.

This evidence suggests the presence of two competing mechanisms of exchange. Figure 12 shows a plot of  $\frac{1}{\tau_B}$  at  $0^\circ\text{C}$  vs.  $[\text{Na}^-]$  and  $\frac{1}{\tau_B}$  at  $0^\circ\text{C}$  vs.  $\frac{P_C}{P_B}$  for the five samples. Again we see the presence of several distinctive trends. Examination of the possible mechanisms shows that a combination of mechanisms A and B could be consistent with this behavior. From Table 6 we have for mechanism A which is



The expression

$$\frac{1}{\tau_B} = \frac{1}{[1 + \frac{k_1 P_B}{k_3 P_C}]} \quad 4.33$$

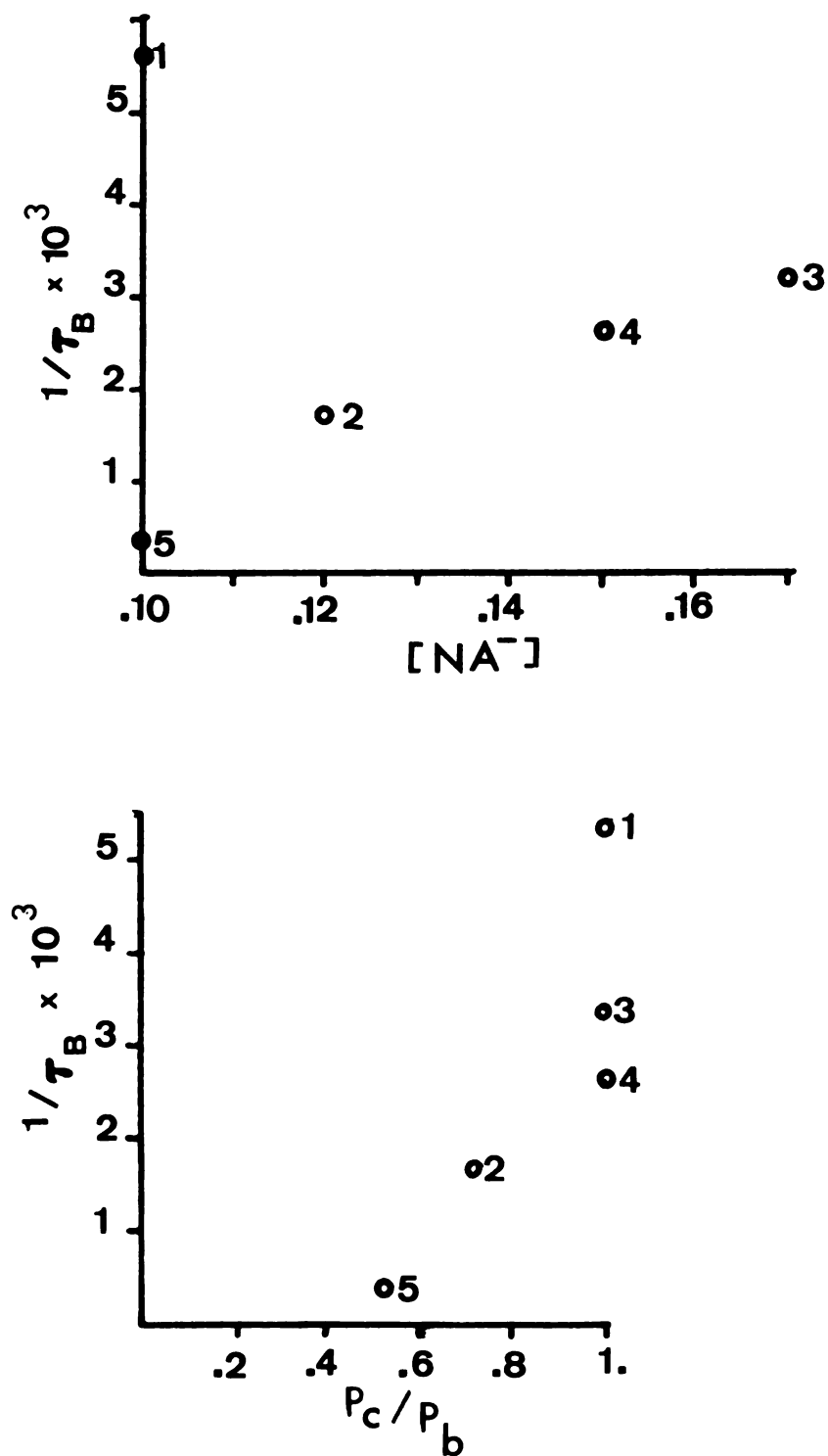
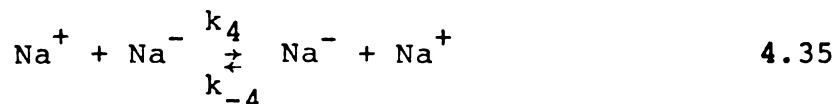


Figure 12. Plot of  $1/\tau_B$  at  $0^\circ\text{C}$  vs (A)  $Na^+$  Concentration (B) Population of  $Na^+$  Site/Population of  $NaC^+$  Site ( $P_C/P_B$ ) for Various Samples.

While for mechanism B which gives exchange via



we have

$$\frac{1}{\tau_B'} = \frac{k_1}{[1 + k_{-1} \frac{(C_T - \text{NaC}^+)}{2k_4(\text{Na}^-)}]} \quad 4.36$$

When A and B are combined we obtain

$$\frac{1}{\tau_B'} = \frac{k_1}{[1 + \frac{k_1 P_B}{k_3 P_C}]} + \frac{k_1}{[1 + k_{-1} \frac{[C_T - \text{NaC}^+]}{2k_4(\text{Na}^-)}]} \quad 3.37$$

$$\text{if } \frac{k_1 P_A}{k_3 P_C} \gg 1 \text{ and } \frac{k_{-1}[C_T - \text{NaC}^+]}{k_4(\text{Na}^-)} \gg 1 \quad 4.38$$

then we have

$$\frac{1}{\tau_B'} = k_3 \frac{P_C}{P_B} + \frac{2k_1 k_4 (\text{Na}^-)}{k_{-1} (C_T - \text{NaC}^+)} \quad 4.39$$

Equation 4.39 predicts that when the concentration of free crown is large,  $\frac{1}{\tau_B'}$  is proportional to  $\frac{P_C}{P_B}$ . When the free crown concentration is small mechanism B dominates the exchange. This would qualitatively explain the variation

of  $\frac{1}{\tau_B}$  with  $\frac{P_C}{P_B}$ . Points 1, 2 and 5 are reasonably linear and could represent the effect of mechanism A. Points 1, 3, and 4 show the effect of excess crown in which case mechanism B would become operative. This assumes that sample 3 which is of high concentration has excess crown present in solution because of solubility limitations on the concentration of  $\text{Na}^+$ . Other experiments are needed in which  $\frac{P_C}{P_B}$  and excess 18-C-6 are systematically varied so that these effects can be studied further.

The results of the 15-C-5 system are very intriguing because of the relatively narrow line of the complex  $\text{NaC}^+$ . This narrow line could be caused by several phenomena. The principal reason for variation in alkali metal NMR line width is the quadrupolar relaxation of the nucleus. This kind of relaxation is dependent on the field gradient about the nucleus. The compound with the larger gradient has a broader line. Therefore, the narrow line in the 15-C-5 system could be because the 15-C-5 has a more symmetrical structure in solution than the other crowns. A second explanation could be that the correlation time is different in the 15-C-5 case. It is not reasonable to believe that the intermolecular motion of the two crowns (15-C-5 and 18-C-6) is different enough to cause this change in correlation time. Therefore, it would require some type of intramolecular motion to cause this difference in correlation times.

This may be a reasonable explanation for the difference in line broadening by crowns and deserves more attention in future work.

## REFERENCES

## REFERENCES

1. J. L. Dye, Pure Appl. Chem., 1 (1970).
2. For discussion of current models of Ammonia solutions, see proceedings of Colloque Weyl IV, J. Phys. Chem. (to be published).
3. J. L. Dye in "Electrons in Fluids", J. Jortner and L. R. Kestner, Ed., Springer-Verlag, West Berlin, 1973, p. 77.
4. S. Matalon, S. Golden and M. Ottolenghi, J. Phys. Chem., 73, 3098 (1969).
5. I. Hurley, T. R. Tuttle, Jr. and S. Golden, J. Chem. Phys., 48, 2918 (1968).
6. J. L. Dye in "Electrons in Fluids", J. Jortner and L. R. Kestner, Ed., Springer-Verlag, West Berlin, 1973.
7. F. J. Tehan, B. L. Barnett and J. L. Dye, J. Amer. Chem. Soc., 96, 7203 (1974).
8. J. M. Ceraso and J. L. Dye, J. Chem. Phys., 61, 1585 (1974).
9. J. C. Petersen, J. Amer. Chem. Soc., 89, 7017 (1967); 92, 386 (1970).
10. B. Dietrich, J. M. Lehn, and J. P. Savvage, Tetrahedron Letters., 2885 (1969); 2889 (1969); J. Amer. Chem. Soc., 92, 2916 (1970).
11. J. L. Dye, M. G. DeBacker, V. A. Nicely, J. Amer. Chem. Soc., 92, 5226 (1970).
12. J. L. Dye, C. W. Andrews, S. E. Mathews, J. Phys. Chem., (to be published).
13. J. M. Ceraso and J. L. Dye, J. Chem. Phys., 61, 1585 (1974).
14. D. E. O'Reilly, J. Chem. Phys., 41, 3729 (1964).
15. D. E. O'Reilly, J. Chem. Phys., 41, 3736 (1964).
16. J. M. Lehn, J. P. Savvage, B. Dietrich, J. Amer. Chem. Soc., 92, 2916 (1970).
17. E. Shchori, J. Jagur-Guodzenski, Z. Luz, and M. Shporer, J. Amer. Chem. Soc., 93, 7133 (1971).

18. E. Shchori, et al., J. Amer. Chem. Soc., 95, 3842 (1973).
19. J. M. Ceraso and J. L. Dye, J. Amer. Chem. Soc., 95, 4432 (1973).
20. J. A. Pople, W. G. Schneider, and H. J. Bernstein, "High Resolution Nuclear Magnetic Resonance", McGraw-Hill, New York, NY, 1959.
21. J. M. Ceraso and J. L. Dye (1974).
22. For example, S. O. Chan and L. W. Reeves, J. Amer. Chem. Soc., 95, 670 (1973); J. Amer. Chem. Soc., 95, 673 (1973).
23. Pat Smith, M. S. Thesis, Michigan State University, East Lansing, Michigan, 1975.
24. V. A. Nicely and J. L. Dye, J. Chem. Ed., 48, 443 (1971).
25. Fred Tehan, Ph.D. Thesis, Michigan State University, East Lansing, Michigan, 1975.
26. I. Langmuir, Phys. Rev., 2, 329 (1913).
27. S. Goldman, R. G. Bates, J. Amer. Chem. Soc., 94, 1476 (1972).
28. G. N. Lewis, M. Randall, B. S. Pitzer, and L. Brewer, Thermodynamics, p. 503, 523. McGraw-Hill Book Co., New York, 1961.
29. J. M. Lehn, Struct. Bonding, (Berlin), 16, 1 (1973).
30. T. C. Waddington, Adv. Inorg. Chem. Radiochem., 1, 157 (1956).
31. C. J. Moody and J. D. R. Thomas, J. Chem. Ed., 42, 205 (1965).
32. M. R. Arshadi, J. CFTAR., 70, 1569 (1974).
33. J. L. Dye, C. W. Andrews, and S. E. Mathews, J. Chem. Phys. (to be published).
34. E. Shchori, et al., J. Amer. Chem. Soc., 93, 7133 (1971); 95, 3842 (1973).
35. J. M. Ceraso, J. L. Dye, J. Amer. Chem. Soc., 95, 1958 (1973).
36. C. Deverell, Progress in Nuclear Magnetic Resonance Spectroscopy, 4, 235 (1968).

37. J. L. Dye, P. Smith, S. Landers and J. Ceraso (to be published).
38. M. Herlem and A. I. Popov, J. Amer. Chem. Soc., 94,  
1431 (1972).



MICHIGAN STATE UNIVERSITY LIBRARIES



3 1293 03082 2179